Spatiotemporal dynamics in the acoustic backscatter of plankton and lesser sandeel (*Ammodytes marinus*) in the North Sea measured using a Saildrone

Sakura Komiyama

Master of Science in Fisheries Biology and Management

Department of Biological Sciences

University of Bergen

June 2021

Supervisors:

Dr. Espen Johnsen, Institute of Marine Research, Bergen

Dr. Geir Pedersen, Institute of Marine Research, Bergen

Professor Arild Folkvord, University of Bergen

Acknowledgements

In writing this thesis I have been blessed by excellent support and guidance. Please accept my sincerest gratitude.

My first and deepest gratitude goes to supervisor Dr. Espen Johnsen for invaluable feedback on my manuscript, the constructive discussion about my thesis at length and guiding me in the right direction.

I also wish to show my gratitude to Dr. Geir Pedersen for the insightful comments about acoustics and assistance with the LSSS software.

Furthermore, I would like to show my appreciation to Professor Arild Folkvord for his incredibly fast replies to my many and vast inquiries and his ever reliable advice regarding writing in a scientific manner.

The assistance and feedback provided by the above-mentioned during discussions have been incredibly insightful and helped me immensely.

I would also like to thank my fellow students that have encouraged me and enabled critical discussion around my work.

Last but not least, I would like to extend my sincere thanks to my family. Without the continuous encouragement and support of my family, this thesis would have never been completed.

Table of contents

Abstract

With accelerating global warming and human activities, the North Sea is one of the marine ecosystems undergoing rapid change. The need for spatially-temporally extendable survey platforms for assisting well-established vessel-based surveys are increasing. In this thesis short term variation in spatial structure of plankton and lesser sandeel (*Ammodytes marinus*) were investigated in the North Sea by using unmanned surface vehicle (USVs) Saildrones equipped with dual frequency (38, 200 kHz) echosounder. The data was collected in two areas, a part of the standard Aberdeen-Hanstholm transect and English Klondyke, an important sandeel fishing ground. These areas were repeatedly covered by two Saildrones in May-June 2019. Repeated surveys witnessed high plankton density in the western part of the Aberdeen-Hanstholm transect constantly during the survey period. Salinity seemed to be one possible factor explaining the heterogeneity of plankton density in both vertical and horizontal structure. Sandeel appeared diurnally at various depths from 2 m to near the sea bottom. There was only a weak tendency that the schools were distributed deeper around midday. However, their diverse vertical distribution indicated underlying drivers of their behaviour other than light. Despite the existing uncertainty of species identification due to lack of ground-truthing and limited frequency availability, this saildrone survey conveyed little but purposeful information of the dynamics in spatial utilization of plankton and sandeel over a short period of time.

Keywords: Saildrone, lesser sandeel, plankton, echosounder, spatiotemporal dynamics, North Sea

1 Introduction

1.1 Ecosystem changes

Climate changes and other footprints of human activity may affect marine ecosystems and the geographical distributions of zooplankton (Beaugrand et al. 2002, Pitois and Fox 2006, Hoegh-Guldberg and Bruno 2010) and fish species (Beare et al. 2004, Perry et al. 2005). One consequence of global warming is earlier spring blooms (Kahru et al. 2011) which impact zooplankton reproduction success (Alheit et al. 2005) and may in turn have ramifications for fish reproduction (Alheit et al. 2005, Régnier et al. 2017). Together with spatiotemporal shifts in fish spawning areas (Bellier et al. 2007, Sundby and Nakken 2008) and timings (Jansen and Gislason 2011) these changes lead to more dynamic and unpredictable ecosystems (Jackson 2008). The accelerating changes in the ecosystem are challenging in many regards. First, the increased level of stressor demands more thorough sustainable management (Piet et al., 2019). Secondly, the continuation of standardized survey time series to monitor the abundance and geographical distribution of fish stocks and zooplankton are not designed to and may not be adequate to examine an ecosystem in change (Breivik et al. in press).

1.2 The North Sea ecosystem

The North Sea is a marine ecosystem characterized by its biological diversity with heavy human activities (Halpern et al. 2015) principally utilized as a fishing area (Daan et al. 1990). Over the last 30 years, smaller fish exhibited an increase in abundance while larger demersal fish declined possibly linked to the removal of their predatory fish, a consequence of fishing activity (Daan et al. 2005). The North Sea has been exposed to an increase in water temperature faster than the global average that affects the balance and productivity of the ecosystem (Beare et al. 2004). It is reported that the fish community changes their spatial distribution mostly towards the north (Beare et al. 2004, Perry et al. 2005) and vertical distribution deepened (Perry et al. 2005, Dulvy et al. 2008). The zooplankton community is a foundation of marine ecosystems and it experienced a large-scale latitudinal distribution shift, well documented with cold-water species *Calanus finmarchicus* and substitution by warm-water species *Calanus helgolandicus* (Beaugrand et al. 2002).

Combining human activities and climate change, the importance of ecosystem assessment is steadily more and more recognized (Browman et al. 2004, Pikitch et al. 2004), thusly establishing adequate survey protocols built upon new technologies.

1.3 Underwater acoustic technology

As a non-invasive tool, the echosounder is an indispensable acoustic means that has been widely used to assess the abundance, distribution and behaviour of fish which is essential information for ecosystem-based management (Koslow 2009, Trenkel et al. 2011, Godø et al. 2014). Echosounder transmits a sound pulse from a directional transducer and records the echo, the reflected energy from an object back to the transducer, also known as acoustic backscatter. The difference in density (ρ) and sound speed (c) with the surrounding water is called acoustic impedance ($Z = \rho c$) and triggers the backscatter. The higher impedance difference returns the stronger backscatter assuming the size and shape of the objects are equal, for instance the seabed or a gas-filled fish swimbladder return distinctly strong backscatters. The backscatter strength changes by species (target strength), although sensitively affected by fish size, tilt angle and behaviour, this acoustic property is a scaling factor for converting acoustic backscatter into fish density by species. Accordingly, underwater acoustic technology has been providing substantial information with respect to geographical distribution and abundance of marine organisms (Simmonds and MacLennan 2008).

In the North Sea vessel-based acoustic survey has been carried out regularly to estimate the abundance of herring and sprat since the 1980s (ICES HQ 2018), and of sandeel since 2005 (ICES 2017). One of the limitations of a vessel-based survey is its inability to reasonably gather time series data in fine-scale whereas fish display diel (Hjellvik et al. 2004, Johnsen and Godø 2007), tidal (Embling et al. 2012), and day-to-day (Birt et al. 2012) variation in the assemblage behaviour. Thus, typical standardized vessel-based survey disregards these variations, given that a vessel passes a set of line transects once per cruise. Another major limitation is incomplete coverage of surface area because of the blind zone and fish avoidance (Aglen 1994). The surface blind zone consists of the depth of the keel plus acoustic nearfield (Simmonds and MacLennan 2008) and fish avoidance is a behavioural response towards a perceived threat from approaching vessels (Aglen 1994, De Robertis and Handegard 2013).

As an alternative platform to compensate for the temporal resolution, stationary acoustic survey makes up for the difficulty of vessel-based surveys (Urmy et al. 2012). It provides long and continuous time series of acoustic data, such as seasonal change of backscatter in the water column (Urmy et al. 2012), fish and zooplankton abundance (Trevorrow 2005), vertical

distribution (Benoit-Bird et al. 2009) and behaviour (Solberg et al. 2012). By deploying the transducer upward, it covers the surface layer where vessel cannot insonify. Nevertheless, spatial coverage is sacrificed since the data is collected at a fixed location.

1.4 Towards long term monitoring

To expand spatiotemporal coverage while maintaining the data resolution (Table 1), unmanned surface vehicles (USV) are rapidly developing and has recently entered scientific fisheries research (Verfuss et al. 2019). Furthermore, as opposed to large research vessels, small USVs are usually much quieter and able to enter shallow waters, possess the possibility to reduce fish avoidance and to widen area coverage. USVs are effective vehicles for monitoring marine organisms long term, meanwhile measuring environmental data with continuous GPS positioning (Verfuss et al. 2019).

Table 1. Advantages and disadvantages of acoustic survey platforms in spatial coverage and temporal resolution.

	Spatial coverage		Temporal resolution
	Horizontal	Vertical	
Vessel-based survey	✓	✓	Cost ineffective
Stationary survey	Not designed for horizontal coverage	✓	✓
Saildrone	✓	✓	✓

Saildrone, one such USV, is a wind-solar powered vehicle originally developed to aid traditional vessel-based survey in harsh conditions at high latitudes (Cokelet et al. 2015, Meinig et al. 2015). It has successfully completed long duration surveys (> 100 days) in the Bering Sea collecting acoustic data along with oceanographic data (Mordy et al. 2017, De Robertis et al. 2019). Comparison of acoustic data between Saildrone and a noise-reduced research vessel demonstrated that depth distribution of backscatter detected by Saildrone was shallower than the vessel particularly at night (De Robertis et al. 2019). This implies that Saildrone has potential to significantly reduce the data bias introduced by fish avoidance. Additionally, a shallow keel depth followed by small platform enables it to insonify shallower water column than a vessel, i.e. Saildrone covers from a couple of metres below the surface whereas a vessel needs to exclude the upper 12 m data from subsequent analysis due to the surface blind zone (De Robertis et al. 2019). Including other advantages such as being cost effective and large

payload capacity compared to other USVs (Meinig et al. 2015), Saildrone should be an asset in ecosystem research.

1.5 Ecosystem key-species lesser sandeel and zooplankton

In view of ecosystem research, small forage fish which are generally planktivorous and short lived species contribute to the balance of the ecosystem due to the dynamic and susceptible fluctuations in the population size through the feed web (Fauchald et al. 2011, Engelhard et al. 2014). One of the most dominant forage fish in the North Sea is the lesser sandeel (*Ammodytes marinus* , Raitt, 1934, hereafter referred to as sandeel) (Engelhard et al. 2014), a small eel-like planktivorous forage fish that can reach a body length up to 25 cm (Reay 1970). Like the other forage fish, it plays a central role in the North Sea ecosystem being the major prey of many top predators, including piscivorous fish, seabirds and marine mammals (Furness 2002, Engelhard et al. 2014). Recently the abundance of sandeel was at an all-time low and the decline in the beginning of the 2000s was in tandem with the climate induced depletion of food availability (Arnott and Ruxton 2002, van Deurs et al. 2009, Lindegren et al. 2018).

Besides being a key component in the ecosystem, sandeels are an important target for industrial fishery since it began in the 1950s and the yearly landing once reached over 1 million tonnes in the late 1980s (Furness 2002). Taking the depression of sandeel abundance, the unregulated fishery was altered by more regulated seasonally areal limited fishery (Lindegren et al. 2018). Some fishing grounds in the northwest North Sea were closed to facilitate the recovery of the sandeel stock and subsequently the breeding success of seabirds (Daunt et al. 2008).

Unlike other pelagic mid-trophic fish species, sandeel displays a unique life cycle and diel behavioural pattern. After metamorphosis, sandeels settle in a sandy substratum and spend most of the year burrowed except for the feeding season from April to July and the breeding season in winter (Winslade 1974a). Even in the feeding season sandeels emerge from the substratum only during daylight hours and are buried at night (Winslade 1974b, Freeman et al. 2004). The amount of emerging fish was observed to change on a daily basis (Freeman et al. 2004). During the feeding season sandeel form dense schools whose size range from a few metres to >1km (Johnsen et al. 2017). Frequently, parts of the schools are connected to favourable sandy substrata, whereas the pelagic part seem to feed closer to the surface (Johnsen et al. 2017). Due to the high affinity to a sandy substratum after settlement, the geographical

distribution of sandeels is patchy and migration between areas are limited (Jensen et al. 2011, Wright et al. 2019) (Figure 2.3).

Sandeel diet in the larval stage is largely dependent on zooplankton, mainly copepods, whose abundance affects the sandeel population dynamics (Arnott and Ruxton 2002, van Deurs et al. 2009, Régnier et al. 2017). Specifically, the abundance of *Calanus finmarchicus* in February, which is the hatching period of sandeels, showed a positive correlation with recruitment of sandeel (van Deurs et al. 2009). The diet in the mature fish is dependent on copepods but larger individuals also feed on conspecific larvae or juveniles (Eigaard et al. 2014).

1.6 Sandeels and plankton as acoustic targets

In the initial development stage of fishery acoustic technology, sandeel was not the main target of acoustic survey since they lack a swimbladder. With higher frequencies however, which have better detection of small and non-swimbladder fish, sandeel became a target species in acoustic surveys in the last two decades.

Freedman et al. (2004) observed a detailed diurnal pattern of sandeel in the water column employing an echosounder. The acoustic observation revealed the day to day variation in the density of diurnal emergence (Freeman et al. 2004). Our accessibility to sandeel in the water accelerated new discoveries. There is an unmistakable relationship between their emergence and temperature of the bottom where they burrowed (van der Kooij et al. 2008). Acoustic surveys with multiple frequencies enable both intraspecific and interspecific classification. Relative value of acoustic property between 4 frequencies (18, 38, 120 and 200 kHz) of small 1-year age groups are distinctively different from those of large 2-year age groups (Johnsen et al. 2009). In the same way, the sandeel schools were correctly separated from mackerel and herring schools (Zahor 2006). Experimental studies for measuring the acoustic properties such as target strength from an individual fish have been performed on sandeel (Thomas et al. 2002, Yasuma et al. 2009, Kubilius and Ona 2012), which originally focused on fish with swimbladder as it is a main source of strong backscatter. The ex-situ experiments with simultaneous video recording of free-swimming individuals revealed that a majority swam with head-up tilt angles (Kubilius and Ona 2012). Measured target strength was brought to in situ observations to estimate number of sandeels in a school which form a variety of structures (Johnsen et al. 2017).

Zooplankton has a long history of being an acoustic target (Greenlaw 1979, Pieper et al. 1990) and being separated from fish schools by the benefits of multifrequency echosounder technique (Kang et al. 2002). Due to their dense assemblages, small body size and variation in shapes and materials classifying zooplankton into small taxa from acoustic properties is considerably difficult. Therefore, three acoustic categories based on their anatomical features; fluid-like, hard elastic shelled and gas-bearing (Stanton et al. 1994) are commonly used in the acoustic surveys (Mair et al. 2005, Lavery et al. 2007). In general, gas-bearing zooplankton such as siphonophores contribute greatly to total acoustic backscatter at low frequency while fluid-like zooplankton including euphausiid (e.g. Atlantic krill) and copepods, contribute to acoustic backscatter at higher frequencies (Lavery et al. 2007). Unlike the fish carrying a well reflecting swimbladder, sound speed as well as density contrast with surrounding water is also an important parameter to estimate individual acoustic properties of the three categories (Simmonds and MacLennan 2008). The theoretically estimated acoustic properties were used to identify species composition of backscatter layers presumably formed by mixed zooplankton in the North Sea (Mair et al. 2005). Compared to zooplankton, little attention has been paid to phytoplankton (Trenkel and Berger 2013).

It is valuable to augment our insight of the North Sea ecosystem via sandeel, a linking species between primary and secondary production to upper trophic coupling with its prey, zooplankton, through the acoustic scope. Saildrone equipped with an echosounder facilitate the acoustic observation of short-term variation in species spatial utilization with the advantage of spatially and temporally extended coverages.

1.7 Study objectives

The primary objective of this thesis is to investigate the variation of the spatial structure in acoustic backscatter of plankton and sandeel over 7 weeks in 2019 with an acoustic survey repeatedly covering the same areas by Saildrones.

The study questions are:

- How does the vertical and horizontal density structures of sandeel and plankton change over time, both within a day and within the survey period?
- What environmental factors affect the spatial structures of sandeel and plankton?

- Will the results bring up potential sampling problems in standard vessel-based acoustic survey, and are USVs a part of future acoustic surveys?

To examine the study questions, two study sites in the North Sea were surveyed during the spring bloom period and the main feeding season for sandeel.

2 Materials and methods

2.1 Technical aspects of Saildrone

Two fifth generation Saildrones (SD1031 and SD1032) were used in this study (Figure 2.1). The main components of the vehicles consist of a wing with a height of 5 m, a hull with a length of 7 m and a keel with a draft of 2.5 m. For forward propulsion the wing uses wind power with an assist of a tail that keeps the wing angle towards the wind. Solar panels were mounted on the wing and hull to charge an internal battery suppling electrical power to equipped sensors and navigation system. Saildrones compute safe navigation for tracing pre-scheduled waypoints by autonomously controlling the vehicle against wind and currents. During the cruise, Saildrones are supervised by trained operators and are capable of changing the pre-programmed missions in case that it needs to return to base. Commonly used atmospheric and oceanographic sensors were preinstalled and capable of monitoring data near real-time transmitted via satellite (Figure 2.2).

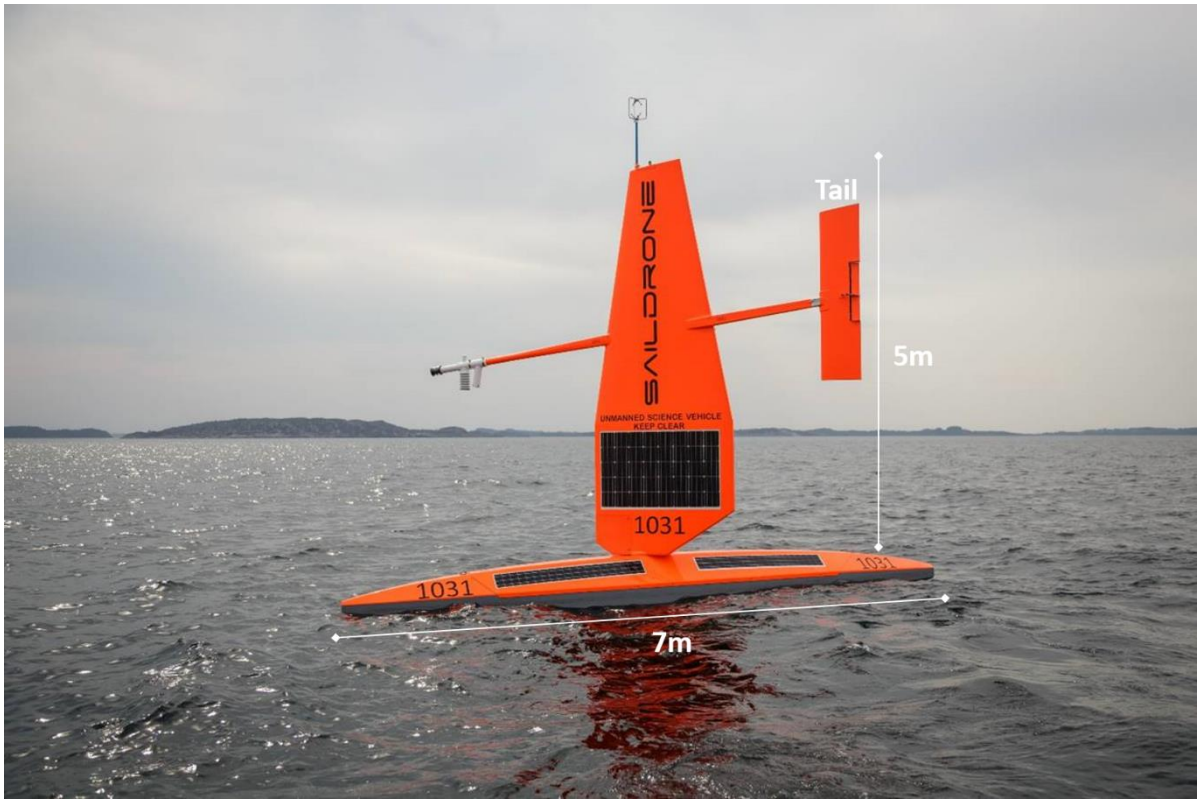

Figure 2.1. Picture of the Saildrone SD1031 taken by Erlend Astad Lorentzen, Institute of Marine Research. Sonic anemometer is visible on the top of the wing, atmospheric sensors (air temperature and humidity sensor and infrared thermometer) and forward camera on the opposite end of the tail.

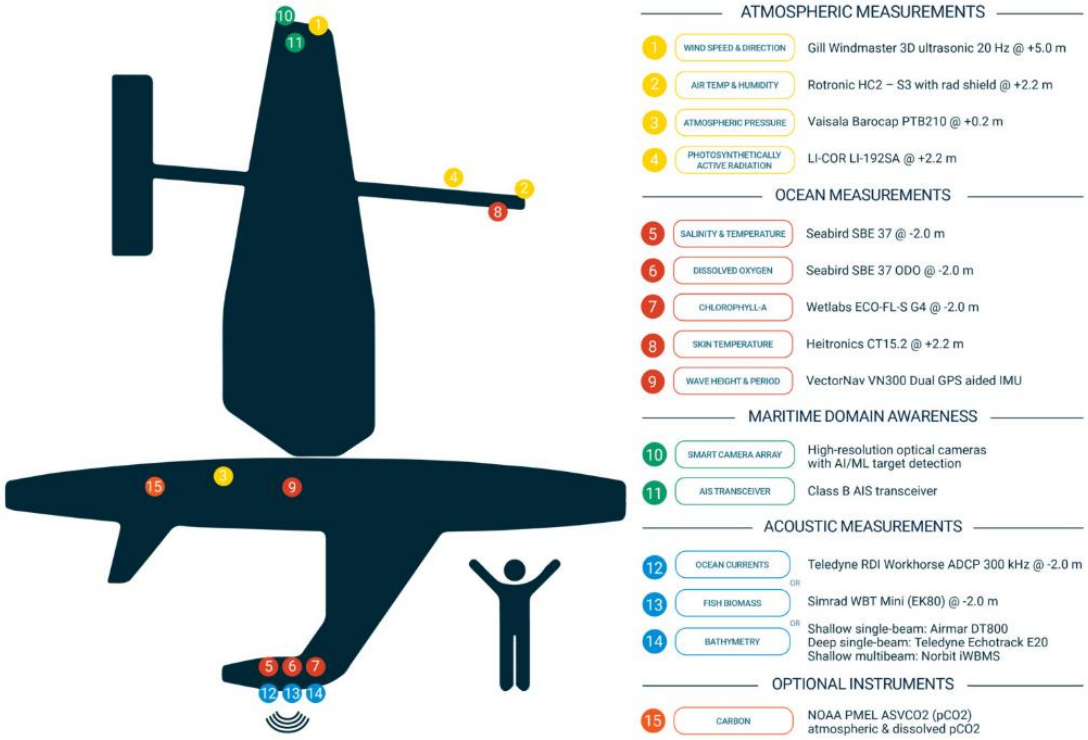

Figure 2.2. Typically equipped sensors and the installed locations (copied from Saildrone, Inc website).

In addition to the basic environmental sensors, an echosounder was integrated to conduct an acoustic survey. A dual frequency transducer, Simrad ES38-18/200-18C (combination of three separate sectors split-beam 38 kHz and single-beam 200 kHz transducers, with a 18° beamwidth), was mounted on the keels about 2 m below the surface. The rolling motion of the vehicles was corrected by mounting the transducer on a gimbal. A wideband transceiver (Kongsberg Maritime Simrad WBT Mini) was installed in the hull.

2.2 Acoustic survey performed by Saildrone

Saildrones were towed by a vessel from Vågen bay, Bergen to Korsfjorden, Vestland and launched into the open ocean on 24 April 2019. After a 121-day survey mission in the North Sea, they were retrieved at the same fjord on 20 August 2019. From the 4-month survey mission completing various tasks, the acoustic surveys conducted at two areas were used in this study (1) a 180 km part of the standard transect between Aberdeen, England and Hanstholm, Denmark (Falkenhaug et al. 2016) (hereafter referred to as the Aberdeen-Hanstholm transect) and (2) English Klondyke, a sandeel bank to assess spatiotemporal dynamics of backscatter

exclusively from plankton (1) and from sandeel along with their prey zooplankton (2) (Figure 2.3). The survey design at English Klondyke was generated using the Rstox surveyPlanner software (Holmin et al. 2019) where the transects followed an equal space zigzag sampler with random starting position (Strindberg and Buckland 2004).

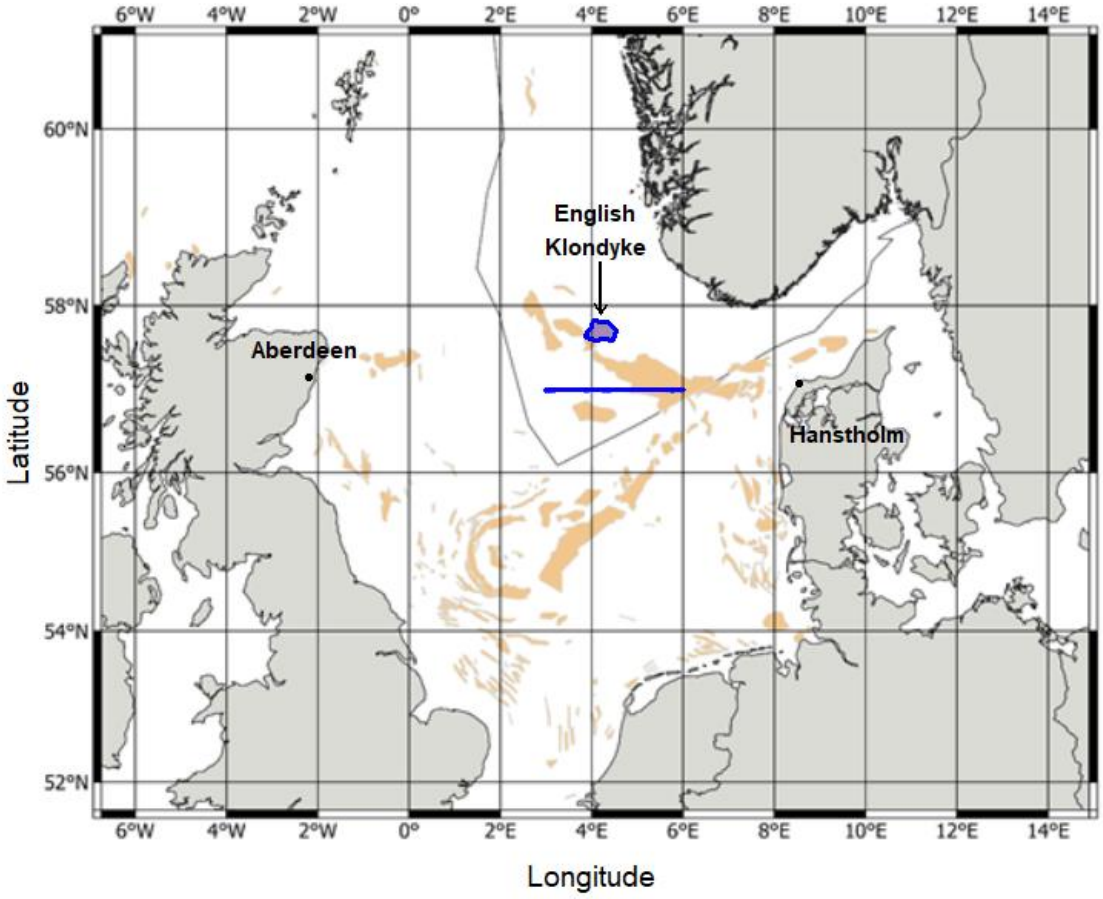

Figure 2.3. Map of the fishing grounds of lesser sandeels in the North Sea (light brown) with the acoustic transects used in this study (blue), modified from a map made by Espen Johnsen, Institute of Marine Research. Transect between Aberdeen, England to Hanstholm, Denmark (Aberdeen-Hanstholm transect) was traced 6 times in total. English Klondyke was covered thoroughly 4 times by utilizing zigzag transect.

The vehicles sailed the Aberdeen-Hanstholm transect from east to west, before returning along the same route to the original starting point. This was run 2 times by SD1031 from mid to late May 2019 (15-20 May and 26-30 May) and once by SD1032 in the beginning of May 2019 (8-11 May), resulting in a total of 6 transects. SD1032 also sailed English Klondyke 4 times from the beginning of May to the end of June (1-3 May, 12-16 May, 12-14 June and 15-20 June) (Table 2).

Table 2. Surveys conducted by two Saildrones. SD1031 sailed the Aberdeen-Hanstholm transect 4 times. SD1032 sailed the Aberdeen-Hanstholm transect 2 times and English Klondyke 4 times intermittently.

	Saildrone	Location	Time (UTC)		Distance (nmi)
1	SD1032	Aberdeen-Hanstholm	08/05/19 11:00 – 10/05/19 01:23	E	125.7
2	SD1032		10/05/19 01:24 – 11/05/19 20:58	W	118.6
3	SD1031		15/05/19 08:00 – 18/05/19 00:16	E	113.2
4	SD1031		18/05/19 00:17 – 20/05/19 05:55	W	108.6
5	SD1031		26/05/19 09:08 – 28/05/19 16:55	E	127.0
6	SD1031		28/05/19 16:57 – 30/05/19 18:49	W	115.5
1	SD1032	English Klondyke	01/05/19 06:59 – 03/05/19 20:57		154.8
2	SD1032		12/05/19 13:00 – 17/05/19 11:57		163.8
3	SD1032		11/06/19 18:01 – 14/06/19 23:53		176.2
4	SD1032		15/06/19 00:02 – 21/06/19 14:57		203.5

E or W: the Saildrones entered the transects from east or west respectively
Entering locations of the English Klondyke coverages are shown in Figure 3.7

During the operation, the location of the Saildrones were monitored via the Saildrone mission portal (https://www.saildrone.com/technology/mission-portal) which also showed low resolution sensors data in real-time.

2.3 Data collection

The equipped echosounders were calibrated at sea off Sandviken, Bergen prior to the mission according to standard sphere method (Demer et al. 2015). While the vehicles were in the target areas, echosounders transmitted a 1.024 millisecond continuous wave every 1.5 second sequentially at 38 kHz and 200 kHz. Echosounders were active 24 hours continuously during the survey with the exception of the period from 1 to 3 May when echosounders were inactive during night from 19:30 to 4:30 UTC to save data storage capacity.

In addition to echosounder data, the Saildrones measured and recorded environmental data simultaneously during the acoustic surveys. All sensors were calibrated before being installed on the vehicles. Data used in this study was wind speed, relative humidity, air pressure, wave period and height, sea surface temperature (hereby referred to as SST), salinity, chlorophyll and oxygen saturation (Table 3). Apart from wave period and height, sensors calculated mean value and standard deviation of the active sampling duration. Mean values were used considering that the variation of acoustic backscatter was the main objective of this study. The

data was downloaded from Saildrone, Inc FTP (File Transfer Protocol) server after uploading directly from the vehicle hard drives post-mission.

Table 3. Environmental data used in this study. Install height indicates the height from sea surface.

Measurements	Install height (m)	Device model	Sampling duration
Wind speed	5.2	Gill WindMaster	60s on, 240s off
Relative humidity	2.3	Rotronic HC2-S3	60s on, 240s off
Air pressure	0.2	Vaisala PTB210	60s on, 240s off
Wave period	0.34	VectorNav VN-300	Always on
Wave height	0.34	VectorNav VN-300	Always on
SST	−0.5	Teledyne Citadel CTD-NH	12s on, 48s off
Salinity	−0.5	Teledyne Citadel CTD-NH	12s on, 48s off
Chlorophyll	−0.5	WET Labs FLS	12s on, 48s off
Oxygen saturation	−0.6	Aanderaa 4831	10s on, 50s off

2.4 Acoustic data processing

For analysing acoustic data quantitatively, the data from the echosounder were first processed with the Large Scale Survey System (LSSS) software version 2.9.0 (Korneliussen et al. 2016), however a software bug was identified during the analyses (see appendix). Thus, the data processing was redone using LSSS version 2.10.0.

To begin with, untargeted water columns such as above transducer and below sea bottom need to be eliminated from the echosounder data since it contains data from a depth that can be arbitrarily set by users which is usually well below the actual sea bottom, up until the surface. LSSS has pre-processing tools called KORONA to set a bottom boundary from an automatic detection of the bottom echoes. One of the KORONA module configuration files "KoronaModuleSetup_Example09_standard" which also detects and removes the ambient noise was used for the process. The created bottom boundary was manually modified after visual inspections to eliminate spike increases of integrated backscatter caused by erroneous detection of bottom echoes. The surface boundary was set to 2.0 m, the depth of the mounted transducers. Data outside of the bottom and surface boundaries were then excluded from subsequent analyses. The water columns containing obvious artificial noise through visual inspection were also excluded from the analysis by defining two vertical boundaries at the outer ends of the water column to enclose this noisy area. By applying an "exclude" tooltip in LSSS, the entire water column both at 38 kHz and 200 kHz within these two boundaries was excluded

from integration of backscattering and data storing. There were two events from English Klondyke data presumed as noise from nearby vessels and its acoustic devices, having a synthetic-like series of pulses exclusively dominating either 38 kHz or 200 kHz.

After the pre-processing, data from the Aberdeen-Hanstholm transect and English Klondyke were scrutinized with different scrutiny methods described in the following subsections. The scrutinized acoustic data was stored by values of the nautical area scattering coefficient (m^2 nmi^{-2}, NASC) by acoustic category with a horizontal resolution of 0.1 nautical miles and a vertical resolution of 1 m and generated ASCII format reports. NASC is a measure of echo energy received from acoustic backscatters in a depth layer where the area covered is standardized to one square nautical mile. In other words, how much echo energy is received from biological organisms if the transmission from the echosounder covered an area of one square nautical mile (Simmonds and MacLennan 2008).

2.4.1 Scrutinizing the Aberdeen-Hanstholm transect acoustic data

In order to examine the distributions of backscatter from plankton (a combination of zooplankton and phytoplankton), both top and bottom threshold was applied to separate the weak targets from the strong targets in the echogram. The top-threshold was set at −55 dB as well as bottom-threshold at −82 dB to cut out signals higher than −55 dB and weaker than −82 dB (Figure 2.4). As a result, top threshold removed the majority of fish schools and bottom threshold removed the majority of background noise. This top- and bottom-thresholding technique was developed to segregate co-occurring fish and jellyfish (Uumati 2013). The backscatter between surface and bottom boundary along entire transect was regarded as plankton in this study.

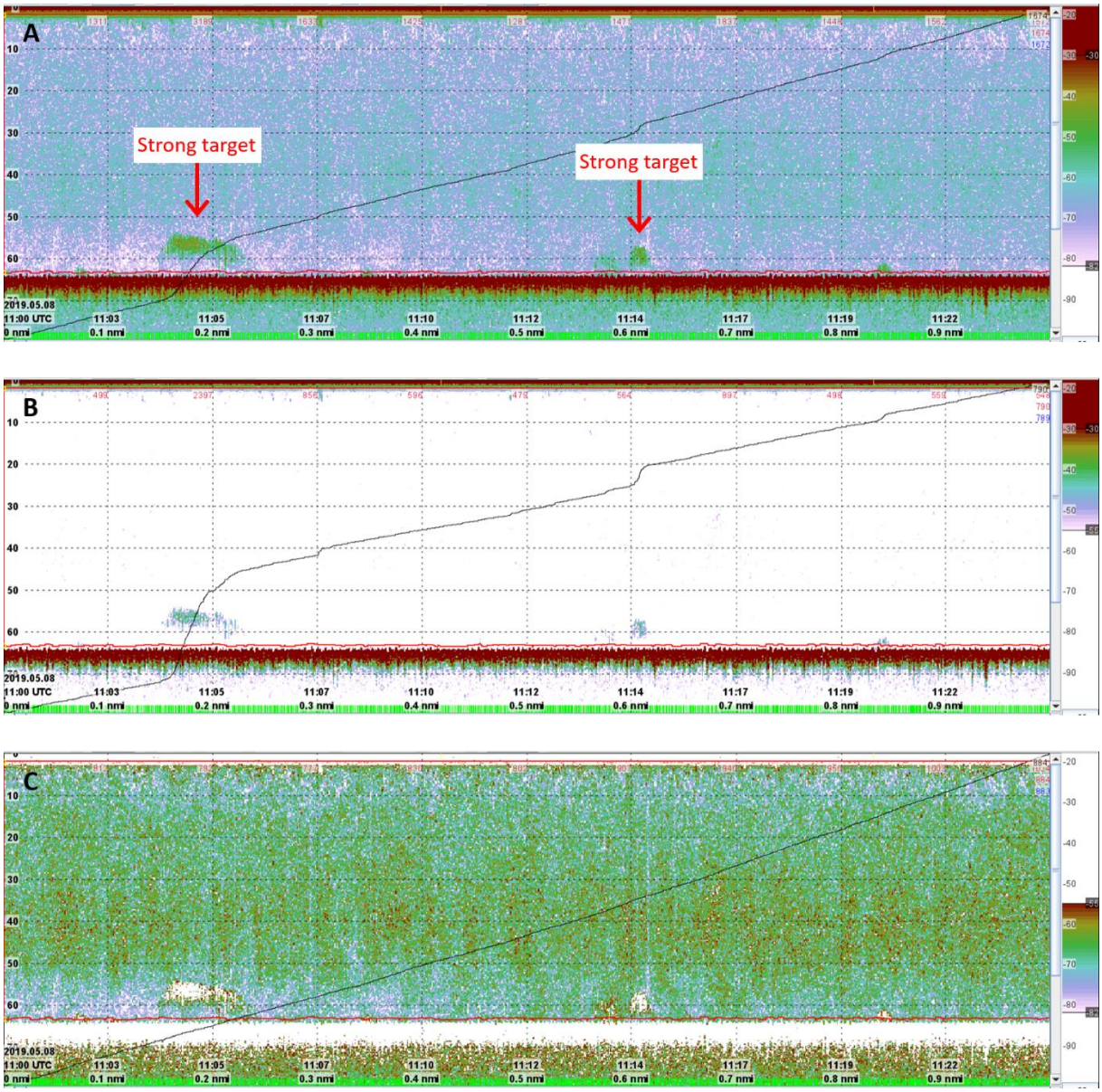

Figure 2.4. An example of 1 nmi echograms from the Aberdeen-Hanstholm transect. The colour scales on the right indicate volume backscattering strength (S_v, dB re $1m^{-1}$). (a) All targets stronger than −82 dB. (b) Only targets stronger than −55 dB by setting S_v threshold at −55 dB. (c) Only targets stronger than −82 dB and weaker than −55 dB by setting top and bottom S_v threshold at −82 dB and −55 dB to exclude targets outside the thresholds.

2.4.2 Scrutinizing English Klondyke acoustic data

The echogram was manually scrutinised mile-by-mile at a threshold of −60 dB. Fish schools were demarcated by the software tool that draws school boundaries automatically at the current threshold. The backscatter of each school box was assigned to 3 categories; “sandeel”, “other fish” and “others” depending on relative frequency response, *r*(*f*). *r*(*f*) is defined as the mean

volume backscattering coefficient of the selected box of a frequency, $\bar{s_v}(f)$ relative to the mean volume backscattering coefficient of 38 kHz, a normalized frequency, $\bar{s_v}(f_N)$, (Korneliussen and Ona 2002).

$$r(f) = \frac{\bar{s_v}(f)}{\bar{s_v}(f_N)}$$

Sandeel schools have unique acoustic characteristics when using 4 frequencies (Zahor 2006, Johnsen et al. 2009) making them almost doubtlessly distinguishable from other categories. Since the Saildrones were equipped with two frequencies, 38 kHz and 200 kHz, *r*(*f*) in this study was $r(f) = \frac{\bar{s}_v(200kHz)}{\bar{s}_v(38kHz)}$. Therefore, school boxes with *r*(*f*) value higher than 1 were assigned to sandeel (Figure 2.5). Other demarcated boxes with *r*(*f*) value less than 1 (Figure 2.6) and remarkably strong backscatters were assigned to "other fish" and "others" respectively to avoid being erroneously assigned to the background which comprises of mostly plankton, partially gas bubbles and negligibly small fish schools. This non-demarcated background backscatter was assigned to a category called "non-schooling targets" at a threshold of −82 dB. The categories "sandeel" and "non-schooling targets" were used for subsequent analyses.

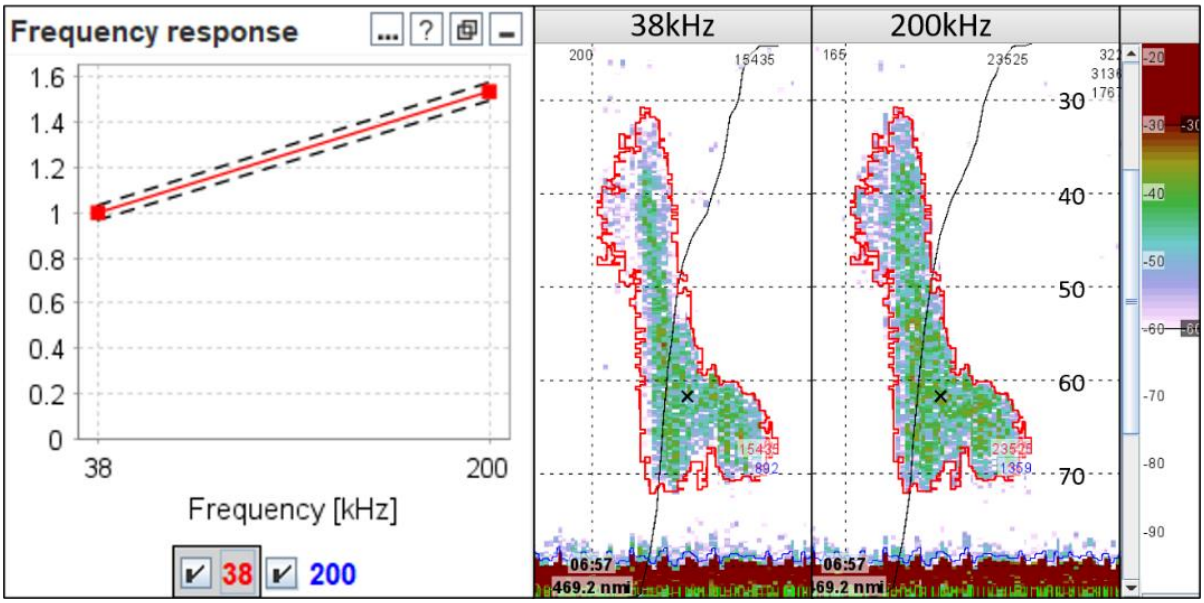

Figure 2.5. An example of a sandeel school at 38 kHz and 200 kHz. Frequency response of 200 kHz is about 1.5. The colour scales on the right indicate S_v (dB re $1m^{-1}$), set to −60 dB to create school boxes.

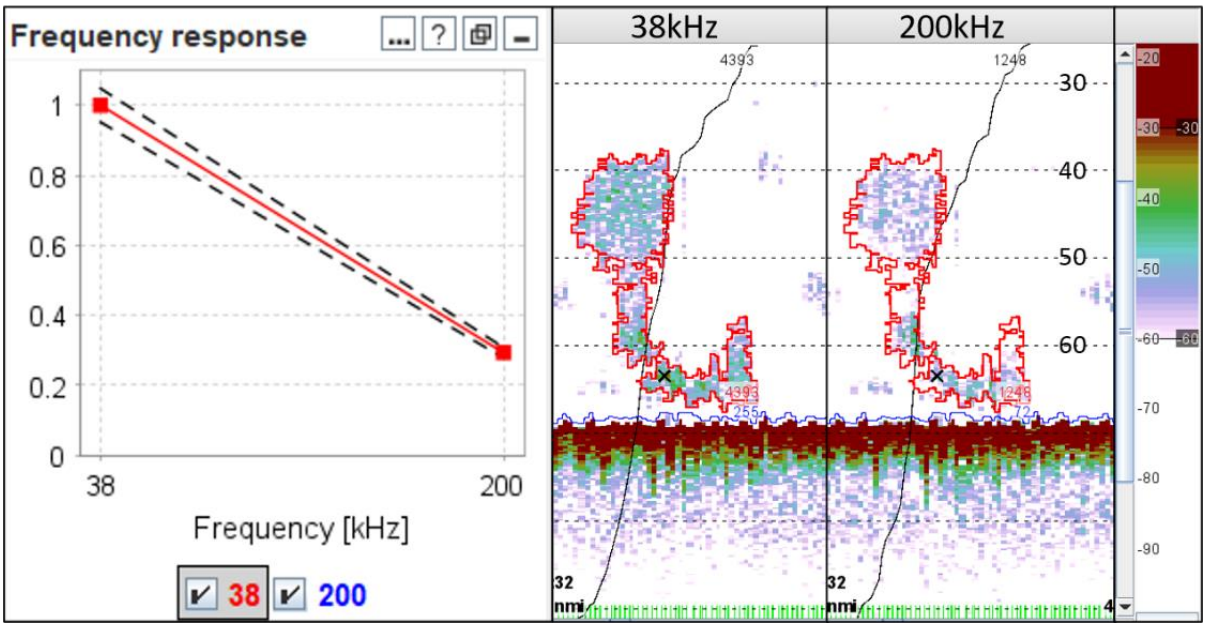

Figure 2.6. An example of a school from other pelagic fish at 38 kHz and 200 kHz. Frequency response of 200 kHz is about 0.3. The colour scales on the right indicate S_v (dB re $1m^{-1}$), set to −60 dB to create school boxes.

2.5 Environmental data

A total of 9 environmental measurements were used to investigate the relationship with acoustic backscatter (Table 3). Wind speed was measured in a vector, that carries wind speed and direction. Horizontal wind speed (*ws*) was calculated by northward (*v*) and eastward (*u*) wind vectors by using Pythagorean theorem (Mauder and Zeeman 2018).

$$ws = \sqrt{(v^2 + u^2)}$$

Two measurements, chlorophyll and wind speed (from the anemometer) failed to collect sufficient number of samples during the survey in English Klondyke. As a countermeasure of the sample numbers of wind speed, estimated wind speed was calculated from Saildrone cruising speed by utilizing the strong linear relationship between them. Saildrones are propelled by wind power. The coefficients of the simple linear regression (β_1 and β_2) were calculated from all available samples combining the Aberdeen-Hanstholm transect and the English Klondyke data. No specific conversion was applied to the other measurements.

2.6 Analysis of spatial and temporal variation in acoustic backscatter

As both zooplankton and sandeel reflect more backscatters at 200 kHz than 38 kHz (Zahor 2006, Lavery et al. 2007, Johnsen et al. 2009), data from 200 kHz were primarily used in the following statistical analyses. For investigating the temporal variation in spatial structure of

NASC, the data was classified into temporal groups, 6 transects at the Aberdeen-Hanstholm transect, 4 coverages at English Klondyke were used as the temporal groups (Table *2*).

In addition to visual interpretation of the scrutinized echograms, inferential statistics was applied to gain further understanding on spatiotemporal variation of the echograms objectively. The subsequent statistical analyses were performed in R (v4.0.4). All statistical processes were applied to 3 categories; (1) the weak targets which removed backscatter stronger than −55dB from the Aberdeen-Hanstholm transect, (2) the non-schooling targets and (3) sandeel schools from English Klondyke. Sandeel NASC containing zero values were removed from the analyses for the reason that those substantial proportion of zeroes violate the assumption of statistical analyses (Fletcher et al. 2005).

2.6.1 Analyses of horizontal distribution

Analysis of covariance (ANCOVA) was carried out for investigating horizontal distribution. The vertically accumulated NASC which was originally stored at a 1 m depth bin every 0.1 nmi was used. The variance of NASC was tested with spatial covariates, longitude or latitude, between temporal groups (6 transects at Aberdeen-Hanstholm or 4 coverages at English Klondyke). Interaction term was included to detect heterogeneity of the covariance between the groups. NASC values were log transformed as the values showed approximately log normal distribution to meet the assumption of the test. The R base function “lm” and 95% confidential interval as significance level were used. Pairwise comparison post hoc test was performed using package “emmeans” (Lenth 2021) when ANCOVA derives significant interaction effect between the temporal groups.

When executing statistical approaches on spatial data, examiners must be aware of probable spatial autocorrelation. Geographically close observations tend to possess similar values than observations far apart in relation to the locomotive capability of organisms. This generates pseudo-replication thereupon type I errors in statistics (Legendre 1993). These pseudo-replications violate the assumption of most standard statistical approaches, independence of observations (Legendre 1993). Acoustic data which depicts NASC values as a two-dimensional plane in high resolution exhibit spatial autocorrelation between samples. In order to mitigate the autocorrelation effect, the samples were averaged every 2 nmi whereas initially stored at 0.1 nmi.

2.6.2 Analyses of vertical distribution

To investigate vertical distribution, weighted mean depths were calculated as:

$$weighted\ depth = \frac{\sum_{i=1}^{n} NASC_i d_i}{\sum_{i=1}^{n} NASC_i}$$

where d_i is a depth at *i*th data sample corresponding *i*th NASC. Weighted mean depth is a representative depth of NASC in vertical distribution by taking mean depth which skews towards the higher NASC. The weighted mean depth was compared with solar altitude, an indicator of time of day as done by Johnsen & Godø, (2007). Solar altitude was calculated in radius for each observation using R package "suncalc" (Thieurmel and Elmarhraoui 2019) and converted into degrees. Hjellvik et al. (2001) introduced a statistical method to evaluate diel variation of bottom trawl catches, where weighted mean depth in this study as a function of solar altitude. The total variations of weighted mean depth at different temporal groups were described as:

$$y_i = \mu_{T(i)} + g(s_i) + \varepsilon_i$$

where $\mu_{T(i)}$ is an estimated weighted mean depth at noon of temporal group $T(i)$, $g(s_i)$ is the function explaining the diel variation, and ε_i is an error term. For the reason that solar altitude carries non-linearity, logistic model was chosen to compute the function $g(s_i)$ after a comprehensive comparison in the previous study (Hjellvik et al. 2001) and defined as:

$$g(s) = \frac{De^{\alpha(s-\beta)}}{1 + e^{\alpha(s-\beta)}} - D$$

here D is the amplitude of diel variation in weighted mean depth, α is the slope (the inclination) of the logistic curve, indicating the speed of diel migrations. β is the midpoint of the curve, indicating when the diel migrations occur (Figure 2.7). Parameter D, α, β were estimated by minimizing the sum of squares using "nls" function in R. Because the final model employs the initial input values of the parameters α and β when the computation does not converge, the function was run multiple times with different initial values until the parameters were estimated by the function. First, the function was applied to the merged datasets (combining all temporal groups). In addition to a model for the merged datasets, a model per individual temporal group was also established to investigate the temporal differences between transects or coverages. For establishing a model of each temporal group, α and β from the merged datasets were applied as initial values of the function and run once, although the computation failed to converge.

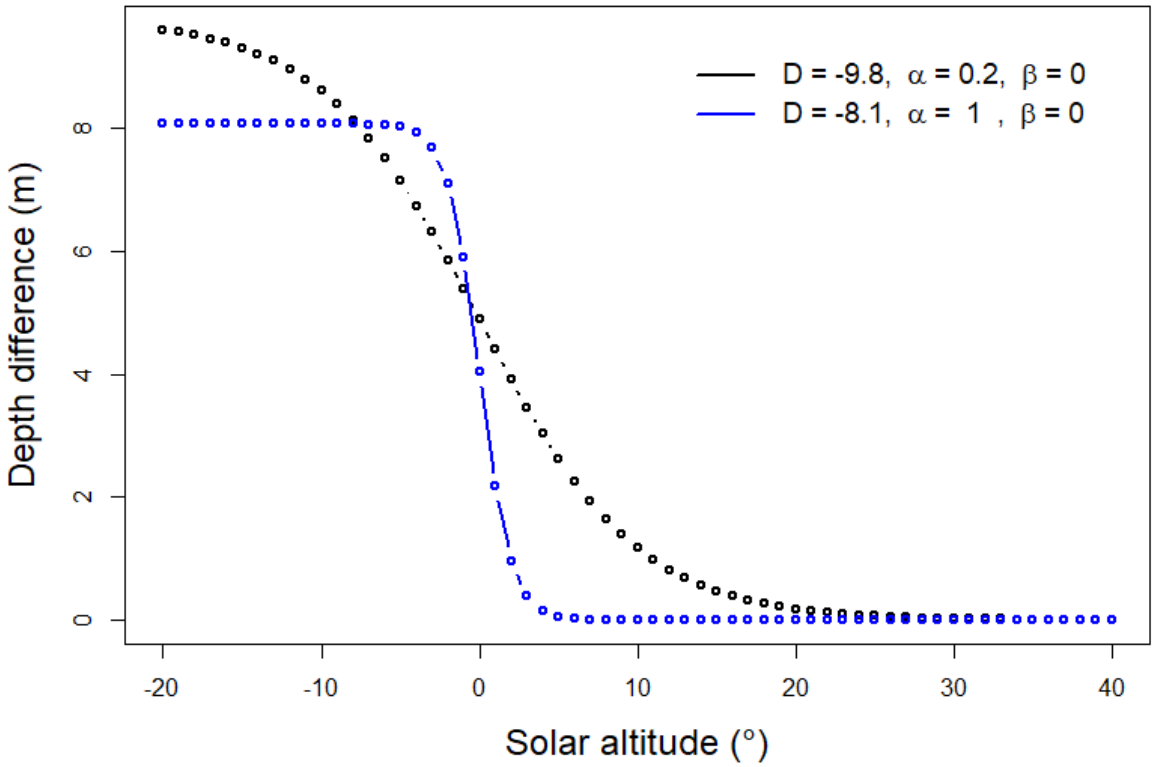

Figure 2.7. A schematic of $g(s)$ function generated from the same dataset. D is the amplitude of weighted mean depth difference. α is the slope of the curve. β is the midpoint of the curve. In this example, the blue line shows a steeper curve (α=1) with 8.1 m shallower at night with two clear levels. The black line shows a less steep (α=0.2) day-night difference without any clear night level. The transitions occur at solar altitude 0° (β) as the centre of the transition in both cases.

2.6.3 The effect of environmental factors on NASC distribution

Lastly, to explore the relationships of the variation in spatial structures (horizontal and vertical distribution represented as mean NASC and weighted mean depth respectively) with environmental factors, multiple linear regression was employed. Stepwise model selection based on AIC via the R base function "step" was used to determine the best model from the 9 available environmental predictors, wind speed, relative humidity, air pressure, wave period and height, SST, salinity, chlorophyll and oxygen saturation (Table 3). The values of predictors were standardized for cancelling the scaling discrepancy between different units and for obtaining a comparable coefficient β between predictors.

3 Results

Throughout the acoustic survey, a strong backscatter layer in the proximity of the surface appeared nearly constantly at the Aberdeen-Hanstholm transect. A similar layer was present in English Klondyke, though appearing rather sporadically. Accumulated NASC values from 0 to 10 m were compared with environmental factors and this layer showed strong positive correlation with wind speed (r=0.75, n=194, p<0.05 and r=0.94, n=77, p<0.05; Figure 3.1).

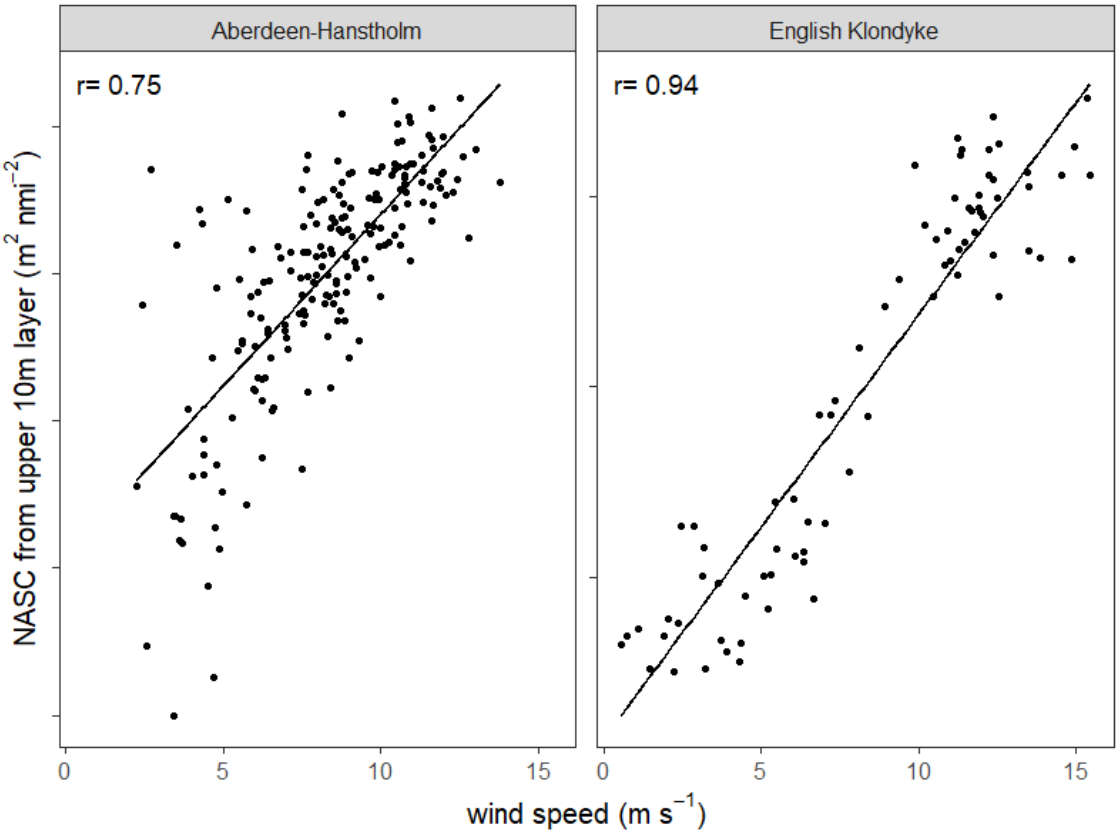

Figure 3.1. Correlation between wind speed and log-transformed NASC of the layer from surface to 10 m at the two study sites with corresponding Pearson correlation coefficients. The NASC of the weak targets at the Aberdeen-Hanstholm transect and the non-schooling targets in English Klondyke were used for the analysis.

Existence of this layer possibly resulted in a phenomenon where wind and organisms intertwined (Trevorrow 2005). In light of the main objective of this study, the impact of the layer would give a false result of the analyses, thus the strong NASC greater than 75% quantile over the datasets were removed from the upper 10 m layer. Subsequent analyses were conducted upon 2 datasets, with and without the strong NASC.

3.1 Aberdeen-Hanstholm transect

Saildrones surveyed the Aberdeen-Hanstholm transect 6 times (hereafter referred to as T1, T2, T3, T4, T5 and T6, respectively) in May 2019 with an average speed of 1.24 ms^{-1} (T1: 1.53 ms^{-1}, T2: 1.30 ms^{-1}, T3: 1.03 ms^{-1}, T4:1.15 ms^{-1}, T5: 1.42 ms^{-1}, T6: 1.23 ms^{-1}). The average wind speed was T1:9.38 ms^{-1}, T2:6.81 ms^{-1}, T3:6.72 ms^{-1}, T4:6.09 ms^{-1}, T5: 8.05 ms^{-1}, T6: 7.17 ms^{-1}.

Overall, mean NASC of each transect were from 286 to 471, the highest at T2 and the lowest at T6. After excluding the strong backscatter from the top 10 m, the mean NASC reduced by 10% to 17%, holding the same trend, T2 the highest and T6 the lowest.

Coupling with a day-night indication, diel vertical migration was observed especially in the west of the transects in the echograms (Figure 3.2), despite the magnitude of the migration being varied between the transects (Figure 3.2). There were strong and thick backscatter layers distributed close to the bottom at T2, T3, T4 and T5 during daytime and weaker backscatter layers at shallow waters during night time notably at T4 around 4.3°E and T5 around 4.5°E. In the east, though clear diel vertical migration was not observed, very thin layers in the shallow water just below the strong backscatter proximity to the surface were observed at T5 and T6. These were assumed as aggregated zooplankton or phytoplankton layers, and the weighted mean depth was greatly affected by the layers. T1 did not exhibit clear vertical migration throughout the transects from the visual interpretation.

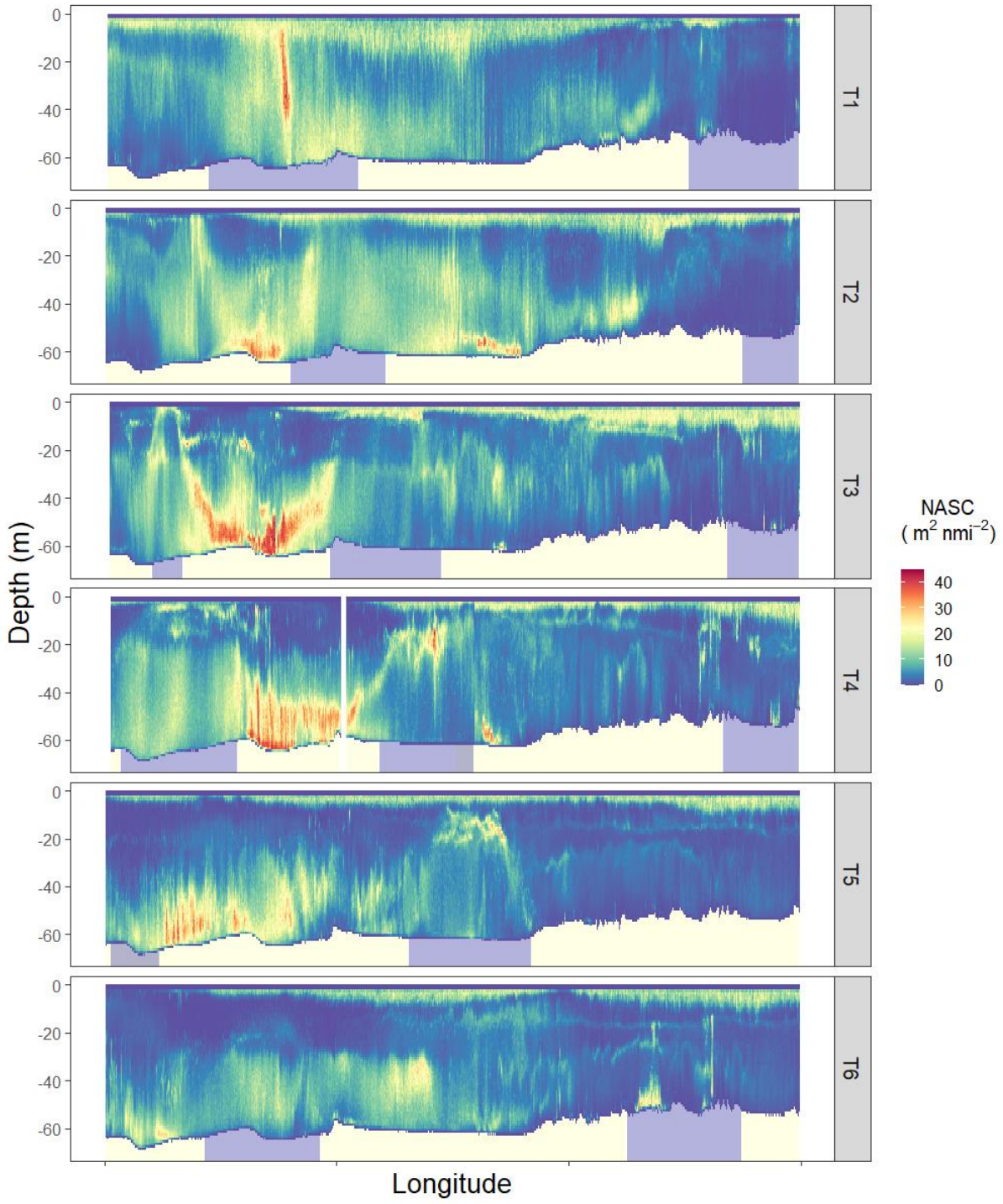

Figure 3.2. 200 kHz echograms of the weak targes (between −55 to −82 dB) at the Aberdeen-Hanstholm transect in May 2019. The backscatter stronger than −55dB were eliminated during acoustic data processing. The colour underneath the echogram shows daytime (light yellow) and night time (light blue).

3.1.1 Horizontal distribution

Horizontal structure of NASC from the weak targets between transects were investigated by ANCOVA and NASC values declined with longitude significantly ($F_{11,330}$ = 48.34, p<0.05),

namely NASC was higher in the west than the east. The interaction between transects and longitude was insignificant after excluding the strong backscatters from the top layer ($F_{5,330}$ = 1.54, p=0.18), thus the westward gradients of NASC were independent between transects. The analysis upon the data including the strong backscatters from the top layers (grey points and lines in Figure 3.3) showed similar trends except for where interaction term was significant ($F_{5,330}$ = 3.68, p<0.05). Pairwise post hoc test revealed that the gradients from west to east at T1 was significantly steeper than at T6 (p<0.05).

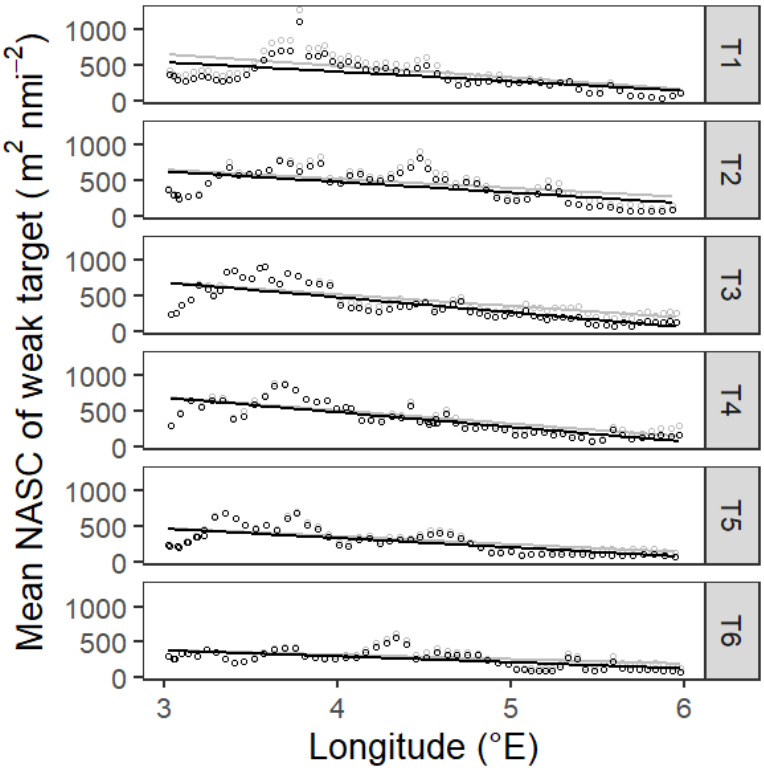

Figure 3.3. Horizontal distribution of NASC from the weak targets at 200 kHz from the Aberdeen-Hanstholm transect measured by Saildrone 6 times repeatedly in May 2019 (T1-T6 respectively), overlayed with the linear regression lines (black). NASC was averaged every 2 nmi (black points) after excluding the strong backscatter at the top 10 m layer. Grey lines and points show the regression lines and the NASC (averaged every 2 nmi) from datasets before excluding the strong backscatter at the top 10 m layer.

3.1.2 Vertical distribution

Visual interpretation of the echogram portrayed thick layers at the bottom during daytime and relatively thin layers in the shallow water during night time (Figure 3.2). These diel vertical variations were examined by logistic model as a function of solar altitude. On account of insensitivity in the calculation of weighted mean depth, 38 kHz was used for the analyses instead of 200 kHz. NASC was overall stronger at 38 kHz, thus weighted mean depth was

dynamically drawn towards the acoustic backscatter layers when compared to 200 kHz. This inferred that weighted mean depth calculated from 38 kHz represented the depth of the layers more accurately.

Model parameters for merged datasets (combining all data from T1 to T6) were estimated by using initial values of 0.5 as α and 15 as β. Estimated parameters did not change dramatically with different initial values. The function behaved steadily. R^2 of the model was 0.09 and each parameter was estimated as; α=0.64, β=−5.77, D=−5.92 (Table 4). In other words, overall vertical migration occurred at −5.77° of solar altitude (corresponding approximately around 2:30-2:50 in the morning and 20:30-21:20 in the evening in May at the study site). The depth at night was significantly shallower than at day with a depth difference of 5.92 m ($p<0.05$)

Table 4. Parameter estimates of diel variation in vertical distribution of the weak targets at the Aberdeen-Hanstholm transect. T1-T6 refers to each acoustic survey repeatedly conducted by Saildrones at the transect while "merged" refers to the overall diel variation from the pooled dataset. Data from 38 kHz was used to estimate parameters. Values in brackets shows the standard error. The second last column shows *p* values of parameter *D*. The last column shows the number of observations. Parameter estimates from datasets after excluding the strong backscatter at the top 10 m layer are only shown.

	α	β	D	μ	R^2	P value	n
Merged	0.64 (0.17)	−5.77 (0.49)	−5.92 (0.35)		0.09	<0.05	6785
T1	0.64*	−9.06 (0.90)	−4.82 (0.43)	34.42	0.12	<0.05	1131
T2	0.07 (0.03)	17.81 (5.00)	−10.57 (3.51)	39.40	0.18	0.003	1051
T3	1.93 (3.21)	−2.25 (0.99)	−3.62 (0.53)	33.71	0.04	<0.05	1246
T4	0.77 (0.57)	−9.16 (1.13)	−6.11 (1.49)	35.82	0.06	<0.05	1100
T5	0.64*	−7.20 (5.37)	−2.01 (1.39)	36.97	0.003	0.147	1110
T6	0.64*	23.32 (0.45)	−15.70 (0.45)	43.78	0.51	<0.05	1147

*the function failed to converge and employed initial values.

Estimated parameters α (0.64) and β (−5.77) were input as initial values to compute parameters for the models of each individual transect. Models for T1, T5 and T6 failed to converge parameter α, thereby employing initial value of 0.64 while the models for T2, T3 and T4 succeeded to compute all unique parameters.

By possessing the highest R^2 value, the T6 model explained the observations with the closest fit (Figure 3.4). Moreover, the depth difference (D) and depth at noon (μ) were the largest among the transects, namely, the NASC layers at T6 showed the most stable vertical migration with the largest depth difference from 28.08 m (43.78 − 15.70) at night to 43.78 m at day. The solar altitude when the migration occurred was also higher than the other transects (solar altitude 23.32° is around 6:20 in the morning and 17:00 in the afternoon in late May at the study site). Unlike T6, the T2 model with the second highest R^2 had a moderate curve which was determined by parameter α (Figure 3.4). The transition speed of diel vertical migration at T2 was slower according to the model. P value for T5 model was found to be not significant (p=0.147), meaning that the depth difference between day and night was not clarified by the model.

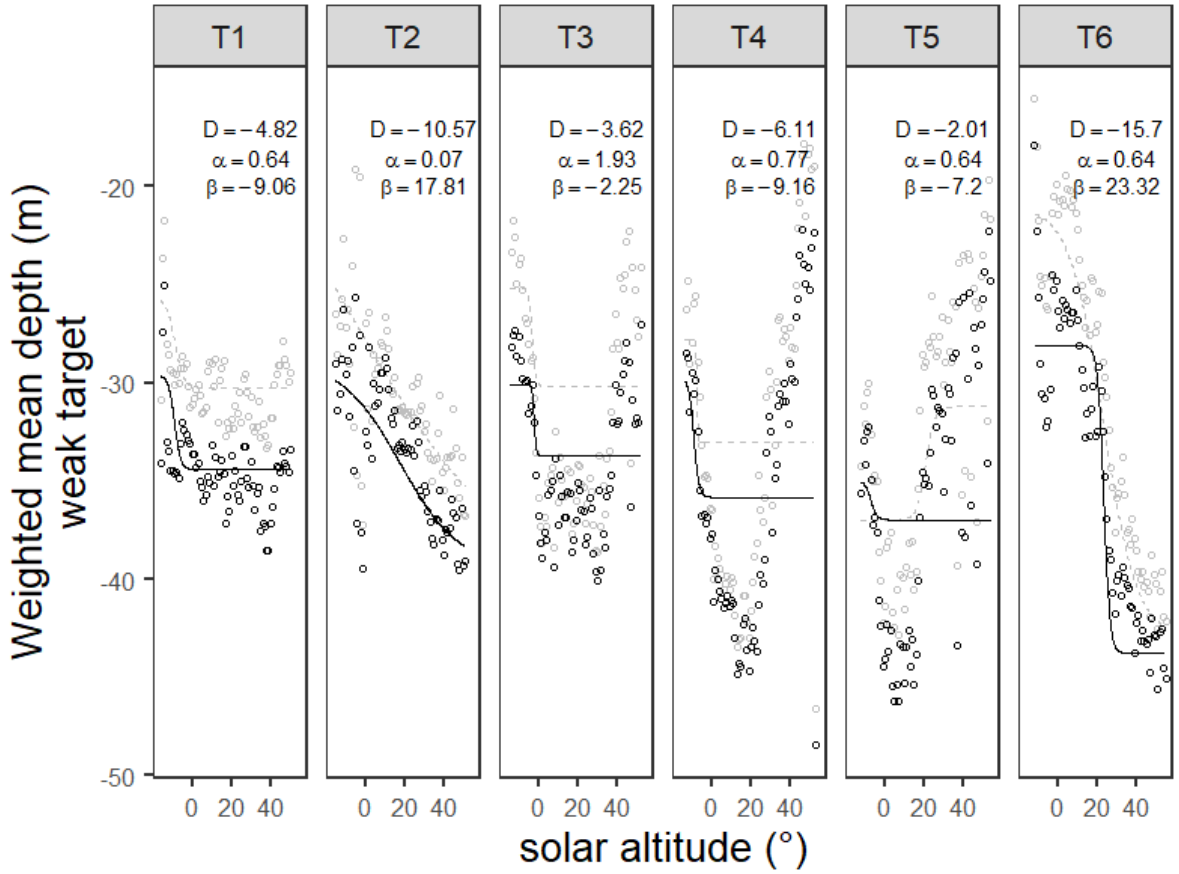

Figure 3.4. Vertical distribution of the weak targets at the Aberdeen-Hanstholm transect measured by Saildrones 6 times repeatedly in May 2019 (T1-T6 respectively) overlayed with fitted logistic models (black solid line) and corresponding parameters. The black points are the median of the weighted mean depth every 1° of solar altitude. Data from 38 kHz was used. Grey dashed lines and points indicate results of the datasets before excluding the strong backscatter at the top 10 m layer.

Noticeably, the observations of T3, T4 and T5 displayed a parabolic pattern, shallow at night, deep at early morning and late afternoon and shallow again at noon. Because of this irregular pattern, the R^2 values of the models for T3, T4 and T5 was low (Table *4*).

As expected, models for datasets including the strong backscatters at the top 10 m layer appeared a few metres above with similar trend barring the model for T5 which had the opposite migration pattern (deep at night and shallow at day) (Figure 3.4). However, the R^2 value of T5 was again one of the lowest among the transects, suggesting that the model did not describe the observations sufficiently.

3.2 English Klondyke

Saildrone SD1032 surveyed English Klondyke in May and June 2019 with the average speed of 0.96 ms^{-1} (May01-03: 1.98 ms^{-1}, May12-17: 0.73 ms^{-1}, June12-14: 1.18 ms^{-1}, June15-20: 0.72 ms^{-1}). The average estimated wind speed was May01-03: 10.91 ms^{-1}, May12-17: 4.44 ms^{-1}, June12-14: 6.84 ms^{-1} and June15-20: 4.53 ms^{-1}.

Total NASC including 4 acoustic categories; sandeel, non-schooling targets, other fish and others (sea mammals or sea birds) were illustrated as echograms by 4 coverages (Figure 3.5). The backscatter in May01-03 and May12-16 were prominently higher than those in June. This was confirmed by a simple one-way ANOVA ($F_{1, 329} = 425.1$, $p<0.05$). In turn, the vertical structure was easily detected by visuals in June while backscatters were distributed extensively with no patterns in May. There were layers of backscatter moving from the bottom to the top in the water column intermittently in June. These layers were assumed as aggregated plankton layers, and the weighted mean depth was greatly affected by the layers. The vertical structures represented by the weighted mean depth were tested in the following subsection. The substantially strong backscatters in the upper layer observed in May01-03 and partially June12-14 was assumed as non-biotic induced backscatter. The numerous ping losses were also recognized from these echograms during the scrutiny process predominantly in May01-03.

Overall, mean NASC of the non-schooling targets at each coverage varied markedly from 221 to 23851, the highest at May01-03 and the lowest at June15-20. After excluding the strong

backscatter from the top 10 m, the NASC was reduced to 98 to 2987, especially June12-14 and May01-03 were reduced by over 85% from the original NASC.

Sandeel had some minute shifts in mean NASC between coverages from 1136 to 2087 (zero values were excluded from the calculation). The NASC fluctuated up and down between coverages or even day to day and displayed no trend in either increase nor decrease along the timeline.

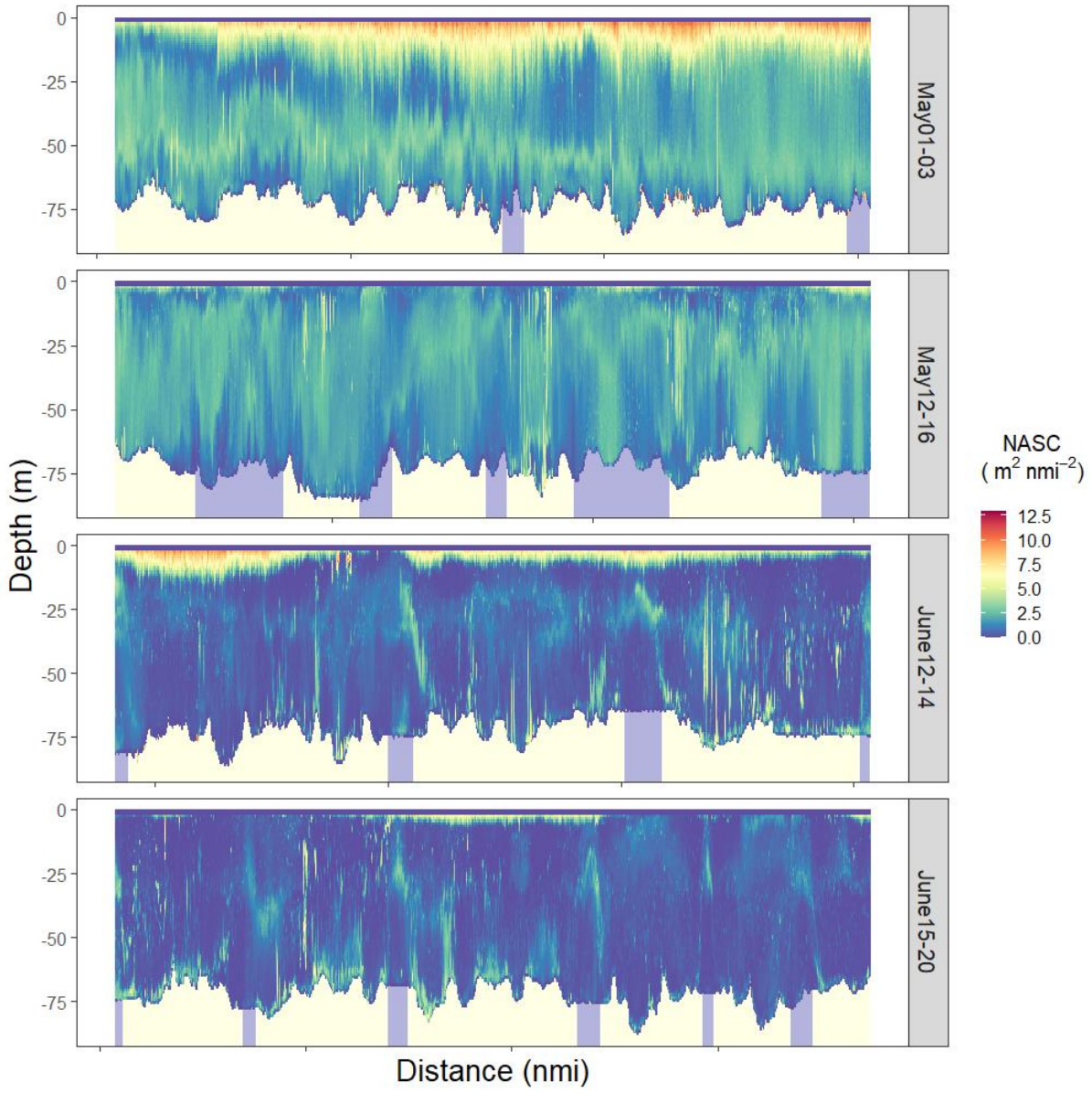

Figure 3.5. 200 kHz echograms of all 4 acoustic categories; “sandeel”, “non-schooling targets”, “other fish” and “others” from English Klondyke measured by Saildrone. NASC values were log transformed as the top threshold was not set and strong backscatter was not separated like the Aberdeen-Hanstholm transect. The colour underneath the echogram shows daytime (light yellow) and night time (light blue).

Sandeel schools appeared during daytime 15 out of 17 days of valid acoustic survey in English Klondyke. Sandeel schools were rarely observed during night time and they appeared right after sunset. Besides, the proportion of these schools was only 1.7% of total NASC from sandeel schools. The schools distributed vertically from 2 m at the shallowest (this is the shallowest depth Saildrones are able to insonify) to 85 m at the deepest, and the pattern of the vertical distribution varied from day to day. For example, most schools ascended close to the surface on the 13 May. Contrarily, most schools stayed below half of the water column from sunrise to sunset on the 13 June, while sandeels were distributed at all depth in the water column on the 16 May (Figure 3.6). This variability of sandeel schools for both horizontal and vertical distribution was attested using statistical approaches (see section 3.2.1 and 3.2.2).

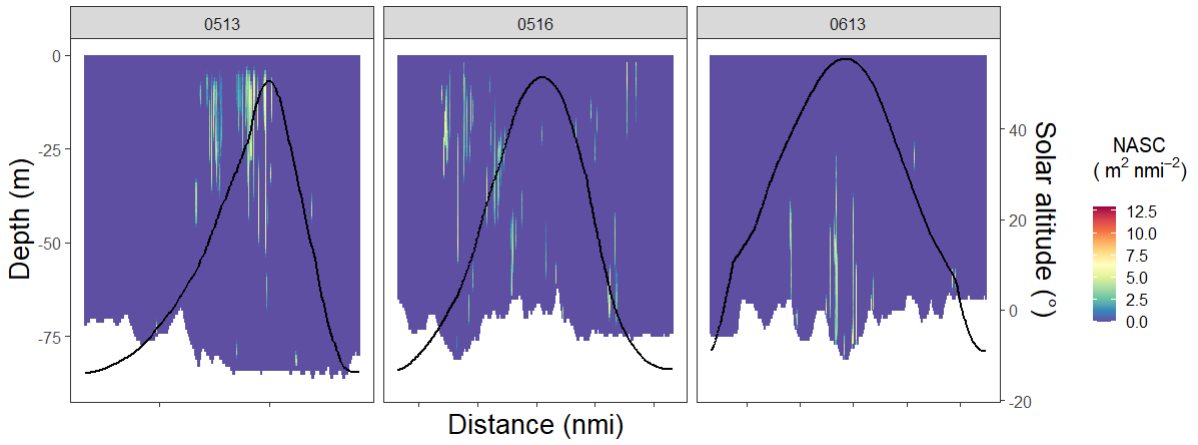

Figure 3.6. Examples of 200 kHz echogram of sandeel (13 May, 15 May and 13 June) in English Klondyke. The black lines indicate solar altitude in degrees. NASC values were log transformed.

3.2.1 Horizontal distribution

Horizontal distribution of non-schooling targets

The horizontal distribution of NASC averaged in 2 nmi is outlined in Figure 3.7. ANCOVA combination with pairwise post hoc test confirmed the positive relationships of latitude and longitude with NASC of the non-schooling targets after excluding the strong backscatters from the top layer. Namely, NASC was higher in northeast than southwest, and the magnitudes of the correlations were dependent on coverages ($F_{11, 319} = 95.93$, $p<0.05$). The interaction effect of latitude was rather faint as the pairwise post hoc test yielded all pairs of 4 coverages insignificant, while the interaction effect of longitude was explicit. 4 pairs were significantly

different from each other according to the pairwise post hoc test. For example, NASC distribution at May01-03 and June12-14 were higher at the east side of the area whereas at May12-16 and June15-20 were almost even from west to east.

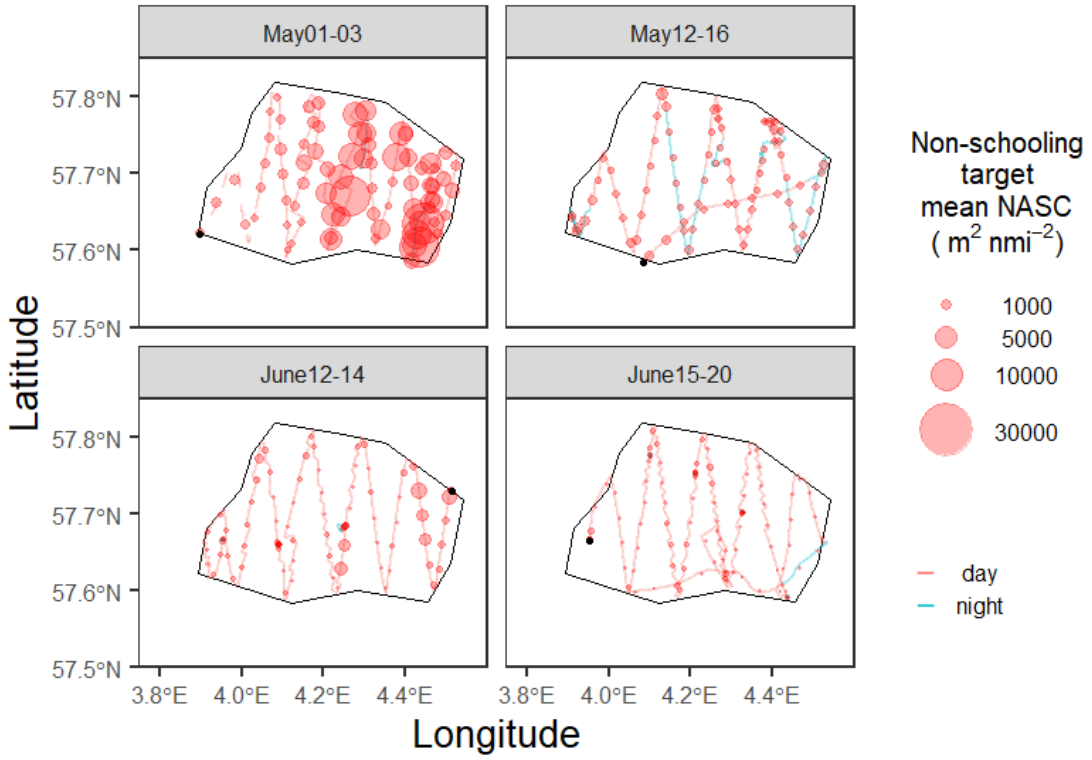

Figure 3.7. Horizontal distribution of the non-schooling targets at 200 kHz in English Klondyke, displaying 4 coverages. Strong backscatters from the top layer were removed. The line indicates the route of the Saildrone with red for daytime and blue for night time. The black points in each coverage indicate the location where the Saildrone entered.

Horizontal distribution of sandeel

As opposed to the non-schooling targets where the variation changed along the longitude, sandeel schools changed its distribution significantly along latitude ($F_{7, 485}$ = 11.82, p<0.05; Figure 3.8). There were more schools in the north than in the south and the magnitude of the gradients were depending on the 4 coverages where May01-03 showed significantly southward distribution compared with May12-16 and June12-14 according to the pairwise post hoc test.

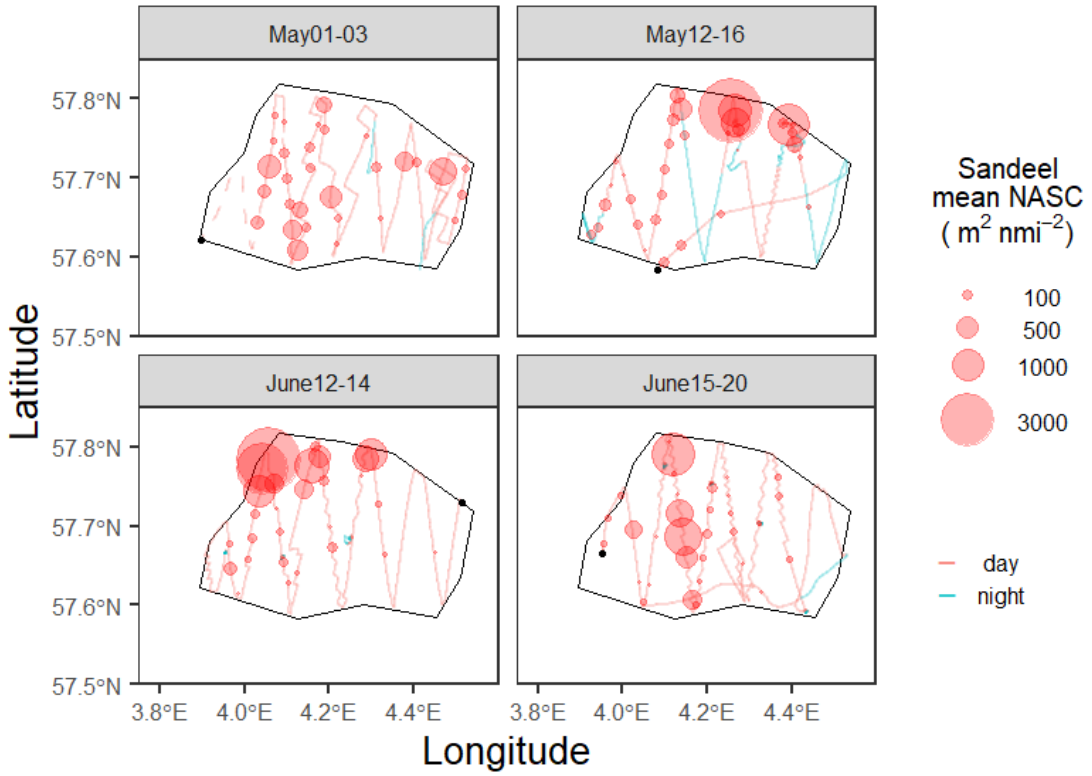

Figure 3.8. Horizontal distribution of sandeel at 200 kHz in English Klondyke, displaying 4 coverages. The line indicates the route of the Saildrone with red for daytime and blue for night time. The black points in each coverage indicate the location where the Saildrone entered.

3.2.2 Vertical distribution

For the same reason as the Aberdeen-Hanstholm transect, data from 38 kHz were used to estimate model parameters for the non-schooling targets. Weighted mean depth calculated from 38 kHz data represented the depth of non-schooling targets more accurately. Contrarily, 200 kHz data were used for sandeel as sandeel has higher NASC at 200 kHz than 38 kHz.

Vertical distribution of non-schooling targets

Initial values of the model for merged datasets (combining all 4 coverages) were 1 and 15 as α and β respectively. The model consisted of relatively high R^2 value (R^2=0.46) and estimated parameters; α=0.37, β=0.19, D=−10.55 (Table 5). Since p value was lower than 0.05, the diel vertical distribution of the non-schooling targets (represented as weighted mean depth) was significantly different between day and night, migrating 10.55 m at 0.19° of solar altitude (corresponding approximately around 3:00-4:00 in the morning and 19:30-20:20 in the evening in the survey period in English Klondyke).

Table 5. Parameter estimates of diel variation in vertical distribution of the non-schooling targets in English Klondyke. "Merged" refers to the overall diel variation from all 4 coverages. Data from 38 kHz was used to estimate parameters. Values in brackets shows the standard error. The second last column shows *p* values of parameter *D*. The last column shows the number of observations. Parameter estimates from datasets after excluding the strong backscatter at the top 10 m layer are only shown.

	α	β	D	μ	R^2	P value	n
Merged	0.37 (0.07)	0.19 (0.59)	−10.55 (0.54)		0.46	<0.05	6383
May01-03	0.20 (0.08)	0.19*	−7.14 (1.39)	26.39	0.02	<0.05	1479
May12-16	0.37*	6.71 (1.59)	−5.85 (0.47)	35.70	0.10	<0.05	1449
June12-14	0.58 (0.25)	−2.71 (0.86)	−12.88 (1.52)	42.18	0.12	<0.05	1621
June15-20	0.43 (0.10)	−1.67 (0.65)	−21.05 (1.58)	49.08	0.30	<0.05	1834

*the function failed to converge and employed initial values.

Individual models for each coverage exhibited some variability in parameters which also influenced the shapes of the models (Figure 3.9). Particularly, June15-20 had large depth difference (21.05 m) with high R^2 value (0.30). According to the model, weighted mean depth of the non-schooling targets migrated from 23.03 (49.08 – 21.05) at night to 49.08 m at day. The migration occurred at the solar altitude of −1.67° (corresponding approximately around 2:35 in the morning and 20:55 in the afternoon in late June).

R^2 values increased from 0.02 to 0.30 with timeline from May to June concurred with an increase of an estimated weighted mean depth at noon, μ (from 26.39 to 49.08 m) and D (from −7.14 to −21.05 m). The trend that higher R^2 accompanied higher μ and D was seen in English Klondyke.

Datasets including the strong backscatters at the top layer drew out models prominently shallower depth at noon (μ) and lesser depth differences (D) (Figure 3.9). The R^2 fell to less than half, meaning the weighted mean depth which was calculated from these datasets were more disorganized and distant from the models.

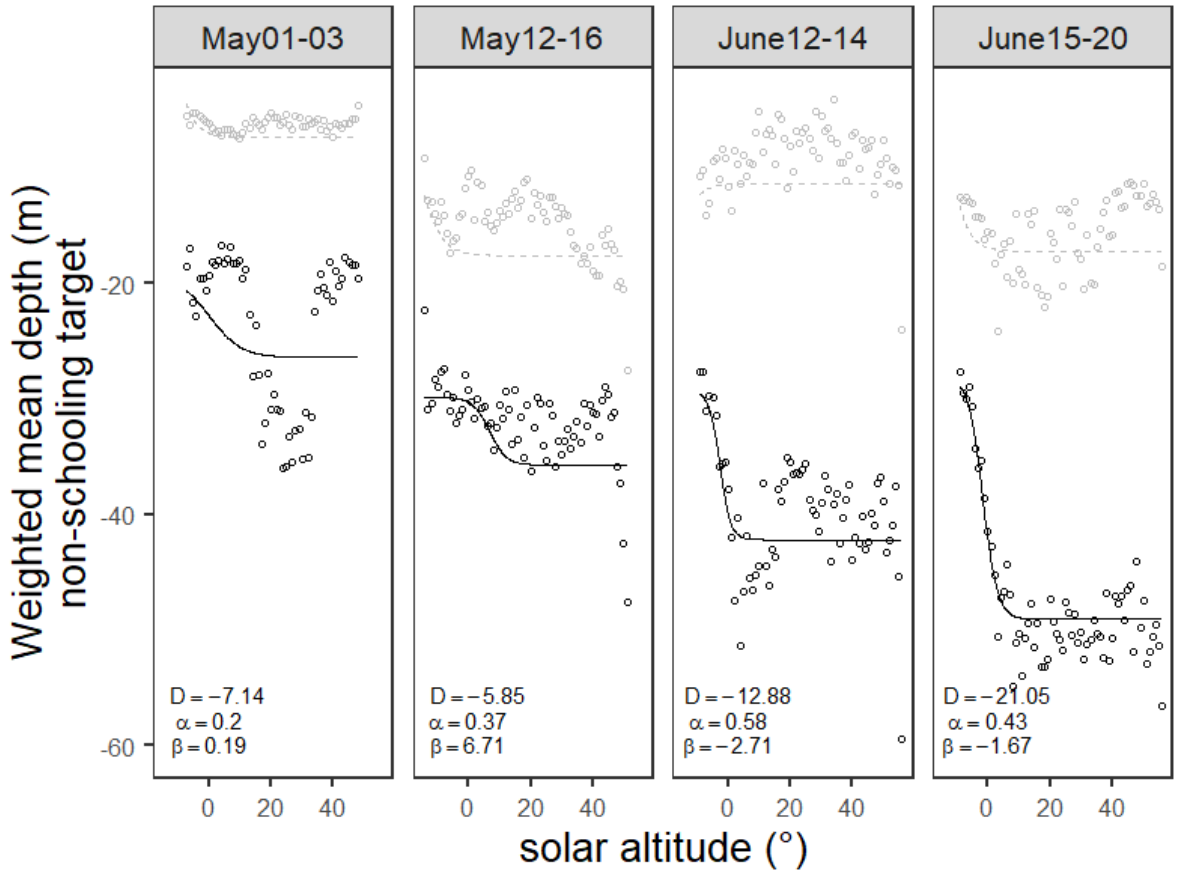

Figure 3.9. Vertical distribution of the non-schooling targets in English Klondyke, displaying 4 coverages overlayed with fitted logistic models (black solid line) and corresponding parameters. The black points are the median of weighted mean depth every 1° of solar altitude. Data from 38 kHz was used. Grey dashed lines and points indicate results of the datasets before excluding the strong backscatter at the top10 m layer.

Vertical distribution of sandeel

The function $g(s)$ failed to converge with tens of pairs with initial values α and β, thereby the model was established with α and β that derived the largest R^2 value of the model and smallest standard error of the parameters. Overall vertical migration of sandeel occurred at solar altitude of 28.03° (corresponding to approximately about 6:45-7:30 in the morning and 15:45-16:45 in the afternoon in the survey period). The depth during morning and afternoon was significantly shallower than during midday with a depth difference of 7.86 m ($p<0.05$) (Figure 3.10). The models for the 4 individual coverages increased the p values of parameter D noticeably, and indeed 2 out of 4 coverages were insignificant (p=0.81 at May01-03 and p=0.43 at June15-20). The vertical distribution of sandeel at these 2 coverages confirmed no significant relationship with solar altitude.

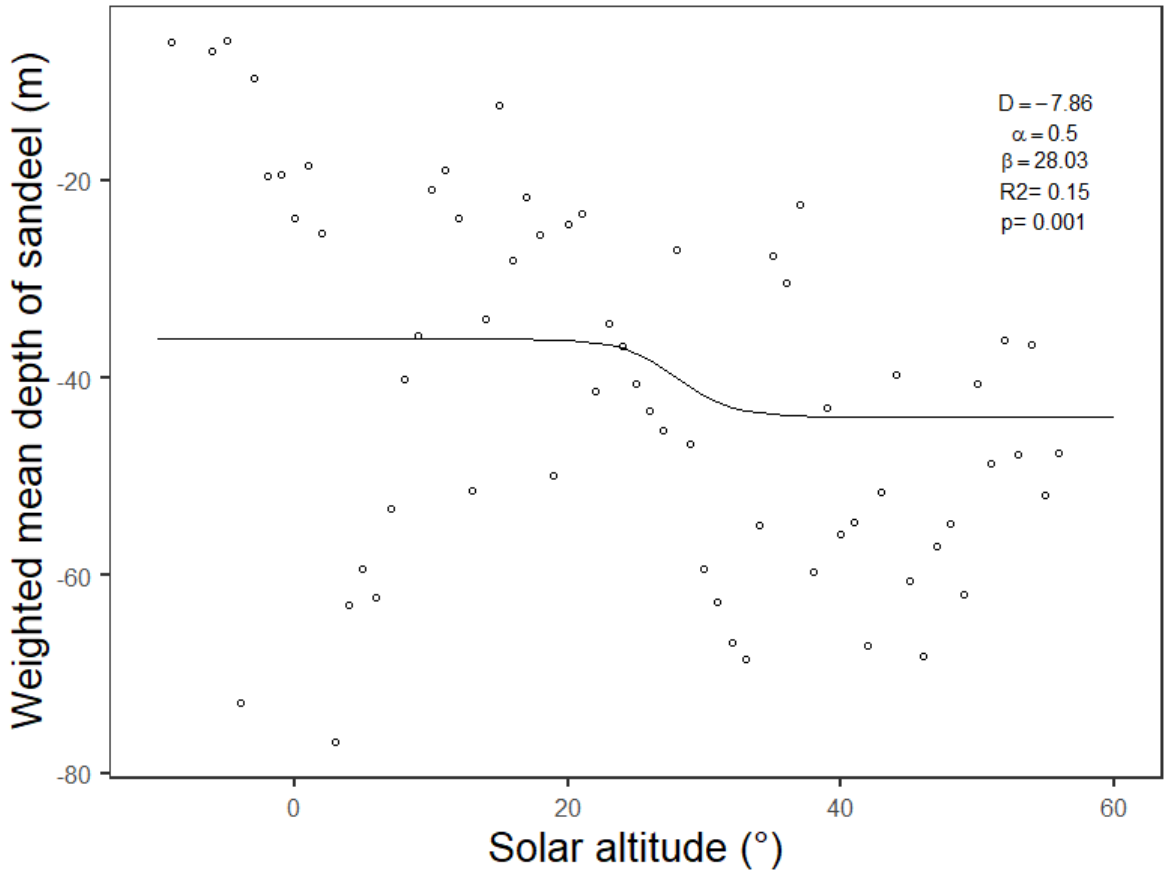

Figure 3.10. Vertical distribution of sandeel at English Klondyke overlayed with fitted logistic models and corresponding parameters. Merged dataset of all 4 coverages were used. The points are the median of weighted mean depth every 1° of solar altitude. Data from 200 kHz was used.

3.3 The effect of environmental factors on NASC distribution

The 9 environmental factors were examined over both vertical and horizontal variations of NASC by means of stepwise multiple linear regression.

At the Aberdeen-Hanstholm transect, 6 factors out of 9 were included in the multiple regression model to explain the horizontal variation of NASC; relative humidity, air pressure, wave period, wave height, salinity and wind speed. The selected model showed a significant positive impact of all variables except for wave height on NASC with R^2 of 0.67 ($F_{6, 107}$ = 39.5, p< 0.05, Figure 3.11). Above all, salinity yielded the highest impact on NASC (β=0.43, p<0.05) followed by relative humidity (β=−0.20, p<0.05).

For vertical variation (represented as weighted mean depth) 7 factors were included in the multiple regression model; relative humidity, air pressure, wave period, SST, salinity,

chlorophyll and wind speed. The selected model showed a significant positive impact of all variables except for chlorophyll on NASC with R^2 of 0.74 ($F_{7, 106}$ = 46.1, p<0.05, Figure 3.12). Above all, salinity yielded the highest impact on the vertical distribution (β=0.87, p<0.05) followed by SST (β=0.52, p<0.05).

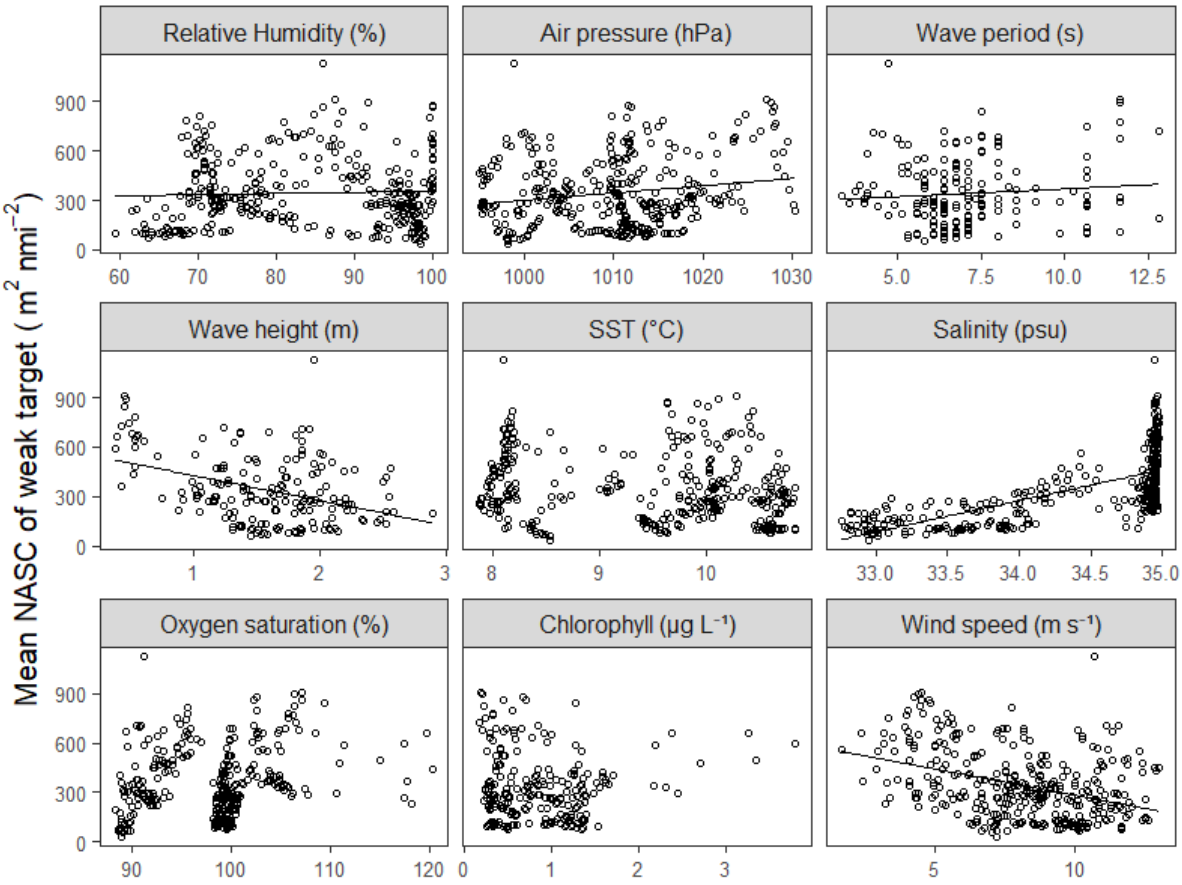

Figure 3.11. Mean NASC of the weak targets (−55 to −82dB) at 200 kHz combining the 6 Aberdeen-Hanstholm transects against 9 environmental factors simultaneously recorded during the acoustic surveys. Factors which were selected via stepwise model selection contains linear regression lines. The dataset without strong backscatter in the top layer was used.

In English Klondyke, there were insufficient samples of chlorophyll. Therefore, 8 environmental factors including estimated wind speed calculated by Saildrone cruising speed were used to find out the best model to explain the variability of horizontal or vertical distribution of NASC.

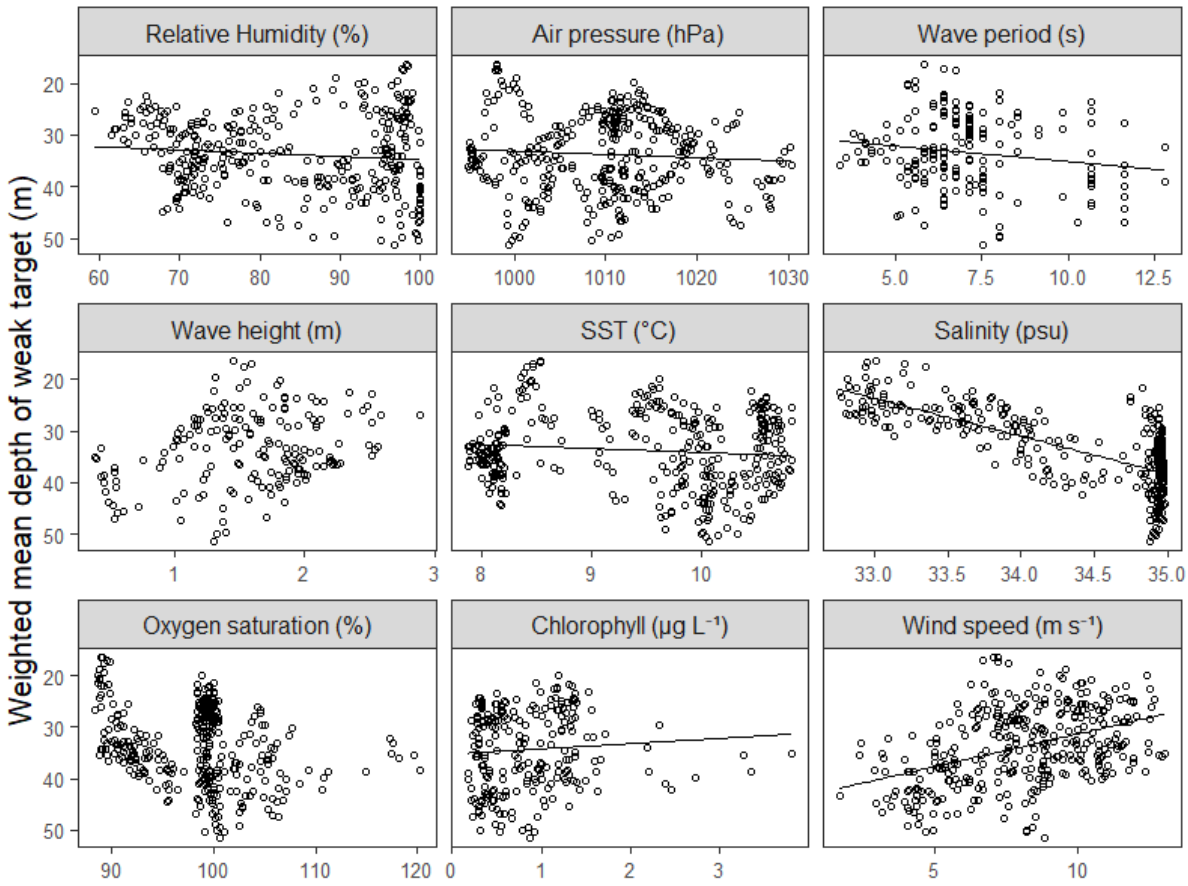

Figure 3.12. Weighted mean depth of weak targets (−55 to −82dB) at 200 kHz combining the 6 Aberdeen-Hanstholm transects against 9 environmental factors simultaneously recorded during the acoustic surveys. Factors which were selected via stepwise model selection contains linear regression lines. The dataset without strong backscatter in the top layer was used.

For horizontal distribution of the non-schooling targets, 5 factors out of 8 were chosen. Relative humidity, wave height, SST, salinity and oxygen were selected as the best model to explain the variation with R^2 of 0.73 ($F_{5, 172}$ = 97.4, p<0.05, Figure 6.4 in appendix). The changes in SST had the highest impact on the NASC variation (β=−0.70, p<0.05) followed by wave height (β = 0.39, p<0.05).

For vertical distribution, 5 factors out of 8 were once again chosen. Relative humidity, air pressure, wave height, oxygen and estimated wind speed were selected to explain the variation with R^2 of 0.19 ($F_{5, 172}$ = 9.38, p<0.05, Figure 6.5 in appendix). The changes in wave height showed the highest impact on the vertical distribution of non-schooling targets (β=−3.40, p<0.05) followed by oxygen saturation (β=−3.35, p<0.05).

For the variation in horizontal and vertical distribution of sandeel, 6 factors and 4 factors out

of 8 were respectively selected as the best model (for horizontal variation: $F_{6,8} = 3.22$, p=0.06, for vertical variation: $F_{4,10} = 7.65$, p=0.004). However, these results left great uncertainty by virtue of the substantially low numbers of degrees of freedom. This was because all zero values in sandeel NASC were removed prior to the analysis to avoid a violation in statistical assumptions (Fletcher et al. 2005).

Table 6. The result of multiple linear regression models to explain the variability of horizontal distribution (represented as mean NASC) and vertical distribution (represented as weighted mean depth) by environmental factors. Environmental factors were standardized and selected via backward stepwise model selection. The predictors are sorted by highest absolute value of β in each analysis. Due to the low degree of freedom, results from sandeel are not shown in the table.

Response	Predictors	R^2	β	*SE*	*P values*
Aberdeen-Hanstholm transect (weak targets)					
Mean NASC	Salinity	0.67	0.43	0.052	<0.05
	Relative humidity		0.20	0.038	<0.05
	Wind speed		0.17	0.062	<0.05
	Wave height		−0.13	0.059	0.02
	Wave period		0.12	0.035	<0.05
	Air pressure		0.10	0.046	0.03
Weighted mean depth	Salinity	0.74	0.87	0.067	<0.05
	SST		0.52	0.160	<0.05
	Relative humidity		0.39	0.077	<0.05
	Air pressure		−0.21	0.061	<0.05
	Wind speed		0.18	0.074	0.01
	Wave period		0.16	0.051	<0.05
	Chlorophyll		−0.14	0.048	<0.05
English Klondyke (non-schooling targets)					
Mean NASC	SST	0.74	−0.70	0.086	<0.05
	Wave height		0.39	0.086	<0.05
	Relative humidity		−0.19	0.080	0.02
	Oxygen		0.14	0.071	0.06
	Salinity		0.13	0.057	0.03
Weighted mean depth	Wave height	0.19	−3.40	1.03	<0.05
	Oxygen		−3.35	0.79	<0.05
	Relative humidity		2.23	0.79	<0.05
	Est wind speed		1.94	0.99	0.05
	Air pressure		1.42	0.80	0.08

To summarize the effect of environmental factors on the spatial structure of NASC, salinity exhibited the highest effect on both horizontal and vertical distribution at the Aberdeen-Hanstholm transect (Table 6). The effect of salinity was relatively small in English Klondyke which was altered by the negative effect of SST and wave height for horizontal and vertical distribution respectively (Table 6).

4 Discussion

By sailing over the same area multiple times, the short-term variation in diel vertical migration of acoustic backscatter from the weak targets and the non-schooling targets was observed. The vertical distribution in relation to solar altitude varied significantly within a few days at the shortest to between months at the longest in this survey period. Contrarily, the vertical distribution of sandeel had a relatively weak relationship with solar altitude despite a perseveration of their diurnal emergence was corroborated by scrutinized acoustic data. Horizontal distribution was on the other hand more stable than the vertical distribution throughout the survey period.

The spatial structure of acoustic backscatter changed dynamically, especially in vertical structure. This short-term fluctuation is generally disregarded by regular vessel-based surveys. Furthermore, data used in this study came from the first comprehensive survey carried out by Saildrones in the North Sea, making the outcomes highly valuable.

4.1 Spatiotemporal distribution of plankton

The acoustic backscatter of the weak targets from the Aberdeen-Hanstholm transects and non-schooling targets from English Klondyke was assumed to be generated by both zooplankton and phytoplankton. These acoustic categories were not completely identical due to the characteristics of the scrutiny method which is discussed in a later subsection (4.4). To elucidate the matter of discussion, the backscatter is regarded as density of plankton consistently in this section.

Horizontal distribution

The horizontal density structure of plankton was comparatively stable over the study period. For the Aberdeen-Hanstholm transect the density was highest in the west with a clear downward trend towards east marking a distinctive boundary at about 4° to 5°E. The horizontal distribution of plankton is primarily governed by hydrodynamics that creates large scale structures such as ocean fronts which in turn form plankton patchiness (McManus and Woodson 2012, Powell and Ohman 2015). The behavioural reactions to horizontal hydrodynamics between zooplankton and phytoplankton are somewhat similar, showing passive drift along the currents or lateral turbulences whereas possessing a vertical swim ability at a speed of 0.1 mm s^{-1} for phytoplankton (Durham et al. 2009) and tens of mm s^{-1} for

zooplankton (Genin et al. 2005). The backscatter boundary observed at 4-5°E in fact overlapped with the area where the salinity level fell, suggesting that the boundary may be a hydrodynamic disruption that elicit a plankton patch. Continuous acoustic observation at the same transect elucidated the different flourishing plankton communities (Powell and Ohman 2015). In English Klondyke, the analysis reflected a significant eastward trend in May01-03 and June12-14. This result is questionable because the coinciding ping loss is a sign of the bad weather conditions (Simmonds and MacLennan 2008, Shabangu et al. 2014), suggesting that the backscatter in these periods were likely not representing the plankton but wind induced bubbles. Accordingly, the horizontal distribution of plankton in English Klondyke was regarded relatively homogenous and did not markedly change during the survey period.

Vertical distribution

Vertical density structures of plankton were found to be more dynamic over time. The depth distribution of the plankton layers was deeper during day than during night, showing the typical diel vertical migration of zooplankton (Tarling et al. 2002). The magnitude of the migration varied from 2.0 m to 15.7 m (analysed from weighted mean depth) between runs of both study sites. The migration occurred basically around sunset and sunrise, however, the timing and speed differed markedly between runs.

Large depth differences showed a consistent clear diel vertical migration throughout the time scale while small depth differences attributed to a cancellation effect possibly from dispersed or inconsistent backscatter distribution. The inconsistency at some of the transects or coverages indicates other related drivers rather than just sunlight. Stationary net sampling studies uncovered a descending behaviour of a copepod species, *Oithona similis* as a response to strong surface turbulences only during night time (Visser et al. 2001). Hydrodynamic shears overwhelm and prevent the vertical movement of phytoplankton which possess limited mobility and form a thin layer for over 12 hours (Durham et al. 2009), often lingering a few metres below the surface (McManus and Woodson 2012). The thin backscatter layers found in the east side of the Aberdeen-Hanstholm transect are replicating these phytoplankton characteristics well. This could also explain the parabolic shape of observations found in some transects. Intrinsically, species interaction and developmental stages lead different vertical migration patterns. For example, 2 common copepod species in the North Sea, *Calanus finmarchicus* and *Calanus helgolandicus* parted their vertical distribution significantly below

and above the water thermocline when they co-occur (Jónasdóttir and Koski 2011). Moreover, a prominent diel vertical migration was seen for earlier developmental stages of *Calanus finmarchicus* while for later developmental stages of *Pseudocalanus elongatus* (Eiane and Ohman 2004).

The transition timings of diel vertical migration were also varied between runs in this study. In general, light is the main driver of the diel vertical migration of plankton. However, apart from changes in daylight hours approaching summer, biological interaction especially predator avoidance was considered and investigated as another driver to modify the timing of diel vertical migration (De Robertis 2002, Tarling et al. 2002). The large scale diel vertical migration of plankton is governed mostly by light intensity (Tarling et al. 2002), yet the timing of the migration in local scale may show variations depending on plankton communities.

The effect of environmental factors

The analysis with environmental factors verified the changes in the physical conditions affected the spatial structures of plankton for both the Aberdeen-Hanstholm transect and English Klondyke. For the Aberdeen-Hanstholm transect, salinity in particular was strongly correlated with both vertical and horizontal distributions. It has been monitored that two closely related zooplankton species had opposite responses to the salinity changes, consequently separating their niches (Lindegren et al. 2020). The result of this study and the behavioural characteristics from previous studies emphasizes the substantial environmental impact led by salinity on the spatial structure of plankton communities in the northern part of the North Sea.

The dominant environmental factor in English Klondyke was SST with a negative correlation against the horizontal variation of plankton. The impact of long term SST change was broadly studied as a factor of latitudinal distribution and community changes of plankton (Beaugrand et al. 2002, Alvarez-Fernandez et al. 2012, Harris et al. 2014). However, this local geographical variation may not directly be explained by SST fluctuation. Instead, with rising SST in June the density of plankton declined significantly compared to May. The seasonal cycle of plankton abundance is a more plausible explanation for the strong negative correlation between SST and density of plankton (Halsband and Hirche 2001). The vertical variation on the other hand exhibited little correlation with environmental factors. Considering that the environmental changes at the Aberdeen-Hanstholm transect greatly affected the vertical distribution of

plankton, the differences in scrutiny methods may ascribe the result. This is discussed in subsection (4.4).

This study conveyed a small indication that diel vertical migrations of plankton are not simple homogeneous events even at the same location and relatively short term (Greenlaw 1979). The magnitude of community diversity (Eiane and Ohman 2004, Jónasdóttir and Koski 2011, Powell and Ohman 2015) in combination with their local physical condition (McManus and Woodson 2012, Lindegren et al. 2020) possibly explain the local dynamics of diel vertical migration of this study. We should nonetheless be aware of that the observation scale of horizontal structure was about 200 times larger than that of vertical structure, making it unsuitable to compare directly (McManus and Woodson 2012).

4.2 Spatiotemporal distribution of sandeel

Horizontal distribution

The analysis for horizontal distribution of sandeel demonstrated a northward trend over time. Conspicuously, high sandeel aggregations found in the coverages May12-16 and June12-14 were static in the northern edge of the area. This result ties well with the latest annual acoustic survey (Johnsen 2019). Considering that the distance between northernmost and southernmost point of English Klondyke is approximately 25 km, the schools were concentrated in the area with the range of maximum 10 km. Based on previous studies (van der Kooij et al. 2008, Johnsen et al. 2017), it is reasonable to assume their home substrata are also in the same area at the northern part of English Klondyke. Although, northward trend was strong during the survey period, school presence in the southern half of the area cannot be neglected. Some schools with relatively high density were observed at the near centre and south of English Klondyke in May01-03 and June15-20. This implies that their emergence rate was lower than the schools in the north. Another driver besides food availability (Winslade 1974c) may be causing the emergence or lack thereof. Water temperature as an additional driver was exhibited having an impact on sandeel emergence (Winslade 1974a). The significant bad weather conditions in May01-03 could potentially contribute to the dissimilarity of sandeel emergence, hence the horizontal distribution as well as the possibility to mask the acoustic backscatter from sandeel schools. Further, every single coverage of this study was comprised of 3-6 days of Saildrone survey, thus strictly speaking it was not snapshot data as was assumed for the

statistical analysis. If schools appeared outside the insonified area, the schools are discounted and neglected from the analyses.

Overall, sandeel distributed along the northern edge of English Klondyke, yet the absence in the other areas could not be verified mainly because of the bad weather conditions in May01-03. Expected density decline from May to June by approaching the end of feeding season was not identified with the data used in this study (van der Kooij et al. 2008). A shift in the age-group of sandeel being consumed by seabirds changed from the 1-year group in the early feeding season to the 0-year group in the late feeding season in the eastern North Sea (Daunt et al. 2008). The demographic structure could compensate each age group and maintain the total sandeel backscatter abundant. However, this does not go beyond speculation as seabirds are able to change its foraging area freely and trawl sampling has evidenced more or less homogeneous demographic structure within a sandeel bank (Johnsen et al. 2009).

Vertical distribution

As previous studies described (Freeman et al. 2004, Johnsen et al. 2017), the sandeel emergence occurred exclusively during daytime in this study. Nevertheless, the vertical distribution was remarkably varied from 2 m at the shallowest to 85 m adjacent to the bottom. Overall depth at dusk and dawn (low solar altitude) were significantly shallower than the depth during midday (high solar altitude). This result is in conflict with previous studies which portrayed sandeel distribution in water column (Freeman et al. 2004, Johnsen et al. 2017), despite the model being a restricted inference from convergence failure of the initial values. Combined with low R^2 values, it was suggested that the relationship between solar altitude and vertical distribution of sandeel was not as solid as it is for plankton. Sandeel primarily follows the light intensity for emerging (Winslade 1974b), whilst vertical locations are likely to be determined by several factors. Two conceivable primary factors for sandeel behavioural decisions should be food and predators. Experimental studies demonstrated an activity depression of sandeel during a food shortage period (Winslade 1974c). At the inshore sandeel bank, they ascend toward the surface with the progressing ebb tide to feed on plankton carried by the tidal current (Embling et al. 2012). Food selectivity has then been closely inspected that sandeel tend to feed on larger size copepods when it is available (van Deurs et al. 2014) and temporal shifting in the prey from plankton to fish larvae was evidenced (Eigaard et al. 2014).

As discussed earlier, the diel vertical migration of plankton possessed heterogeneity to a certain degree and prey dependent depth change can explain the diversification of vertical distribution.

Another major factor is predator avoidance. Their considerably large school formation together with the contact to the bottom is considered as anti-predator adaptation (Johnsen et al. 2017). Predator avoidance behaviour is often unpredictable in responding to predator attacks and displaying flexible decisions sometimes leads to an erratic escape (Zheng et al. 2005). Combining foraging strategies, sandeel depth and perhaps emergence are highly context dependent.

4.3 Using USVs as an acoustic survey platform

This study was a part of a 4-month continuous survey in the North Sea (Johnsen 2019) carried out by 2 Saildrones, unmanned surface vehicles (USVs). USVs extend the total survey period considerably (Mordy et al. 2017, Verfuss et al. 2019) in contrast to the standard survey period of research vessels which is 2 to 5 weeks (Falkenhaug et al. 2016, ICES 2017, ICES HQ 2018). Owing to the lack of biological sampling, USVs cannot be a complete replacement of vessel-based acoustic survey. Still it bears a promising potential to assist those surveys by extending spatial and temporal coverages, favourably in high latitude oceans where a few species often are dominating which may enable identification of said species via acoustic backscatter (Swart et al. 2016, Mordy et al. 2017, Levine et al. 2020).

The outcomes of this study brought up an additional prospect of USV usage. One of the vehicles in this study spent a total of 17 days in English Klondyke where the density of sandeel varied by coverages or even day to day. There were 2 days where the Saildrone did not detect any sandeel schools. Regular vessel-based acoustic survey requires only 1 day to cover a sandeel bank and execute the survey 2 times per cruise (ICES 2017). If the data from the 2-day survey is used to estimate annual abundance and distribution of sandeel, misinterpretation in long-term trend may occur due to ignorance of the short-term fluctuations. Likewise, geographical structures of acoustic backscatter might be overlooked due to lower temporal resolution. Repeated observations in this study found a persistent horizontal gradient in acoustic density at the Aberdeen-Hanstholm transect. A similar structure was confirmed in the sea off California with transect coverages being traced more than 100 times by autonomous underwater vehicles (Powell and Ohman 2015). This intensive repeated survey revealed the

significant differences in community and body size of zooplankton across the boundary (Powell and Ohman 2015). For vessel-based acoustic surveys, witnessing the abrupt ecosystem shift as a result of the thermal threshold of planktonic species (Gregory et al. 2009) have been limited to date. Since the effect of changes in the zooplankton community is substantial on sandeel larvae and other forage and higher trophic fish (van Deurs et al. 2009), survey repeatability should be increased by means of USVs.

4.4 Methodological issues

Scrutiny method

Two different scrutiny methods were used in this study; top- and bottom-thresholding technique (Uumati 2013) for the Aberdeen-Hanstholm transect data and standard visual scrutiny using *r(f)* (Korneliussen and Ona 2002) for English Klondyke data. By comparing the two echograms for each site illustrated in the result section, the surface bubble layers at English Klondyke were profoundly stronger than that of the Aberdeen-Hanstholm transect, after taking that the NASC of English Klondyke data was log-transformed into consideration. Subsequent statistical analyses have also exhibited larger differences between two datasets, with and without the strong backscatter at the top 10 m in English Klondyke. NASC at English Klondyke was more affected by the strong backscatter presumably induced by wind (Simmonds and MacLennan 2008) than the Aberdeen-Hanstholm transect as a result of the scrutiny method. The top- and bottom-thresholding method was not applied to the English Klondyke data because backscatter above the set threshold inside the school boxes were likely to also be removed in the LSSS software. When schooling fish is the target species together with plankton, this regular scrutiny method needs to be used (Korneliussen and Ona 2002, Hjellvik et al. 2004). However, as long as comparison is made within the data come from the same scrutiny method which this study has followed, critical errors are unlikely to occur. This issue in the software may need to be evaluated closely for further applications such as engaging fish and plankton at the same time to investigate prey-predator interaction (Kang et al. 2002).

Need for ground truthing

During acoustic data scrutiny, the researcher proposes the following questions: “What produced the backscatter?” and “How many/much?”. Direct biological sampling such as trawling has been providing the answers to those questions. Catching the suspect answers the first question, and measuring acoustic energy from an individual answers the second question

with some mathematical approaches being applied (Simmonds and MacLennan 2008). In fact, the vessel-based survey conducted in English Klondyke coincided with the Saildrone survey, providing beneficial biological data to answer the questions (Johnsen 2019). Still uncertainties in matching the biological data and acoustic data interpretation remain from various sources throughout the analyses (Demer 2004). For instance, species allocation contributes 60-80% of the biomass estimation error (Simmonds and MacLennan 2008). Although misallocation of sandeel is quite low because of their unique acoustic characteristics (Zahor 2006, Johnsen et al. 2009), increased uncertainty in scrutiny and interpretation caused by no ground-truthing from direct sampling is probably the most significant disadvantage of a Saildrone survey. Further, backscatter layers presumed as plankton in this study remained a matter of conjecture.

Acoustic blind zones

Another well-known limitation of acoustic technique are blind zones at the surface layer and dead zones at the bottom (Aglen 1994). The surface blind zones has been reduced significantly by using Saildrone (De Robertis et al. 2019). De Robertis et al., (2019) first evidenced the reduction of vessel avoidance reaction from walleye pollock (*Gadus chalcogrammus*). The shallowest sandeel schools in this study was observed at 2 m. This is the shallowest observable depth of the Saildrones and cannot be observed by large vessels. Short clearance in conjunction with quiet mechanics of the vehicle undeniably contributed to this new discovery. The dead zone at the bottom was not measured in this study. Contrarily to the surface blind zone, Saildrones are assumed to have a larger bottom dead zone by cause of the transducer beamwidth being wider (18°) than standard vessel mounted transducers (7°). As a countermeasure, the effect can be mitigated by implementing a dead zone correction (De Robertis et al. 2019), though an underestimate of near bottom backscatter should be taken into consideration.

Surface bubbles

Some advantages can be disadvantages in other aspects. A strong backscatter layer in the proximity of the surface was found at both study sites which showed strong correlation with wind speed. Previous research measured bubble attenuation of hull-mounted transducer and drop keel-mounted transducer, and found that mean backscatter of hull-mounted transducer dropped with wind speed over 15 ms^{-1} significantly more than drop keel-mounted transducer (Shabangu et al. 2014). Saildrone transducer which is equipped even shallower showed low

mean backscatter when wind speed was over 10 ms^{-1} (De Robertis et al. 2019). The surface layer observed in our data matched with the previous studies, suggesting it was a bubble layer induced by wind. This surface bubble layer can potentially underestimate the NASC during bad weather conditions, also generating ping losses (Simmonds and MacLennan 2008, Shabangu et al. 2014). To account for the strong backscatter at the surface, a procedure for excluding only strong backscatter (75% quantile) from the layer was applied in this study, but not adequately. The remaining wind induced backscatter made it difficult to separate the abiotic and biotic phenomenon. A better post processing method should be considered for surface bubbles (De Robertis et al. 2019). It should be noted that the effect of surface bubbles on backscatter from sandeel schools was not considered in this study under the assumption that it is not as affected.

The effect of spatial autocorrelation in statistical analysis

To investigate species distribution in general, spatial autocorrelation needs to be accounted for (Legendre 1993). Averaging 2 nmi of original data was done for the horizontal analyses to mitigate the autocorrelation effect. It must be cautioned that 2 nmi spacing was determined subjectively which could be determined by variogram (Maravelias et al. 1996) or Moran's I test (Dormann et al. 2007). Some trials of variogram delivered rather incoherent ranges of lag distance between Aberdeen-Hanstholm data and English Klondyke data. This could also be a result of applying a different scrutiny method.

After the effect of spatial autocorrelation being broadly recognized in the biogeographical field (Legendre 1993), several statistical approaches to account for spatial autocorrelation by including autocorrelation terms in the model have been introduced and has become more prevalent in recent years (Dormann et al. 2007). These approaches should be implemented for utilizing all available information in statistical analyses and may provide a better picture of the data.

Prospects for future progress

Understanding short term fluctuations of species spatial structure will permit detaching it from long-term distribution shifts or phenomena and would ultimately enhance our knowledge of the marine ecosystem. USVs including Saildrones equipped with modern acoustic instruments have potential to disclose underwater life to a large extent both spatially and temporally beyond

the capability of standard research vessels. Lacking ground-truthing and limited frequency availability could be compensated with precise species identification. Sandeel have a species-specific acoustic signature which is distinguishable from others, making it a suitable target species to start with. This study discovered the relationship between solar altitude and the variability in vertical distribution of sandeel, yet their underlying motivation that explains the high variability remains concealed. By means of the new technologies in-depth studies to reveal the underlying motivation should be conducted in the near future.

Conclusions

This study investigated the short-term spatiotemporal dynamics of plankton and sandeel in the North Sea by using echosounder equipped USVs, Saildrones. The acoustic backscatter recorded by the vehicles exhibited some heterogeneities in the spatial utilization of the species.

The diel vertical migration of acoustic backscatter primarily from plankton changed notably between runs over the 7-week survey period, in spite of a typical pattern being confirmed from a significant correlation with solar altitude. The horizontal structure of acoustic backscatter was comparatively stable and a persistent boundary appeared at 4-5°E at the Aberdeen-Hanstholm transect, indicating a possible change in planktonic community structure. The environmental factors explained a large extent of the variation in spatial structure especially for the Aberdeen-Hanstholm transect whose data was well separated between weak and strong targets showing strong correlation with salinity in particular. In line with previous studies, sandeel schools emerged exclusively during daytime at the northern edge of English Klondyke. The vertical displacement only had a weak correlation with solar altitude, shallow in the morning and the afternoon, and deeper in the midday. Otherwise, the vertical locations were vastly spread in a water column without distinct patterns, suggesting underlying biological drivers other than light.

The shallowest detected sandeel school during the survey was 2 m, an unobservable depth for large vessels. Nevertheless, the room for further improvement such as lack of ground-truthing, the effect of surface bubbles and the available frequency limitation remain, though the results of this study highlight the extra aspects of USVs as an acoustic survey platform. In addition to providing longer duration and wider coverage, it also serves as a repeatable survey platform. Understanding the local planktonic and fish communities, distribution and behaviour of the unpredictably changing ecosystems through echosounder installed USVs will fill in the blanks of standard vessel-based surveys.

5 References

Aglen, A. 1994. Sources of error in acoustic estimation of fish abundance. Marine Fish Behaviour (book) in Capture and Abundance Estimation. Fishing:107–133.

Alheit, J., C. Möllmann, J. Dutz, G. Kornilovs, P. Loewe, V. Mohrholz, and N. Wasmund. 2005. Synchronous ecological regime shifts in the central Baltic and the North Sea in the late 1980s. ICES Journal of Marine Science 62:1205–1215.

Alvarez-Fernandez, S., H. Lindeboom, and E. Meesters. 2012. Temporal changes in plankton of the North Sea: Community shifts and environmental drivers. Marine Ecology Progress Series 462:21–38.

Arnott, S. A., and G. D. Ruxton. 2002. Sandeel recruitment in the North Sea: Demographic, climatic and trophic effects. Marine Ecology Progress Series 238:199–210.

Beare, D. J., F. Burns, A. Greig, E. G. Jones, K. Peach, M. Kienzle, E. McKenzie, and D. G. Reid. 2004. Long-term increases in prevalence of North Sea fishes having southern biogeographic affinities. Marine Ecology Progress Series 284:269–278.

Beaugrand, G., P. C. Reid, F. Ibañez, J. A. Lindley, and M. Edwards. 2002. Reorganization of North Atlantic marine copepod biodiversity and climate. Science 296:1692–1694.

Bellier, E., B. Planque, and P. Petitgas. 2007. Historical fluctuations in spawning location of anchovy (*Engraulis encrasicolus*) and sardine (*Sardina pilchardus*) in the Bay of Biscay during 1967-73 and 2000-2004. Fisheries Oceanography 16:1–15.

Benoit-Bird, K. J., W. W. L. Au, and D. W. Wisdom. 2009. Nocturnal light and lunar cycle effects on diel migration of micronekton. Limnology and Oceanography 54:1789–1800.

Birt, M. J., E. S. Harvey, and T. J. Langlois. 2012. Within and between day variability in temperate reef fish assemblages: Learned response to baited video. Journal of Experimental Marine Biology and Ecology 416:92–100.

Breivik, O. N., O. N. Breivik, O. N. Breivik, and E. Johnsen. (in press). Predicting abundance indices in areas without coverage with a latent spatio-temporal Gaussian model. ICES Journal of Marine Science.

Browman, H. I., K. I. Stergiou, P. M. Cury, R. Hilborn, S. Jennings, H. K. Lotze, and P. M. Mace. 2004. Perspectives on ecosystem-based approaches to the management of marine resources. Marine Ecology Progress Series 274:282–285.

Cokelet, E. D., C. Meinig, N. Lawrence-Slavas, P. J. Stabeno, C. W. Mordy, H. M. Tabisola, R. Jenkins, and J. N. Cross. 2015. The use of Saildrones to examine spring conditions in the Bering sea. OCEANS 2015-MTS/IEEE Washington:IEEE.

Daan, N., P. J. Bromley, J. R. G. Hislop, and N. A. Nielsen. 1990. Ecology of North sea fish. Netherlands Journal of Sea Research 26:343–386.

Daan, N., H. Gislason, J. G. Pope, and J. C. Rice. 2005. Changes in the North Sea fish community: Evidence of indirect effects of fishing? ICES Journal of Marine Science 62:177–188.

Daunt, F., S. Wanless, S. P. R. Greenstreet, H. Jensen, K. C. Hamer, and M. P. Harris. 2008. The impact of the sandeel fishery closure on seabird food consumption, distribution, and productivity in the northwestern North Sea. Canadian Journal of Fisheries and Aquatic Sciences 65:362–381.

De Robertis, A. 2002. Size-dependent visual predation risk and the timing of vertical migration: An optimization model. Limnology and Oceanography 47:925–933.

De Robertis, A., and N. O. Handegard. 2013. Fish avoidance of research vessels and the efficacy of noise-reduced vessels: a review. ICES Journal of Marine Science 70:34–45.

De Robertis, A., N. Lawrence-Slavas, R. Jenkins, I. Wangen, C. W. Mordy, C. Meinig, M.

Levine, D. Peacock, H. Tabisola, and O. R. Godø. 2019. Long-term measurements of fish backscatter from Saildrone unmanned surface vehicles and comparison with observations from a noise-reduced research vessel. ICES Journal of Marine Science 76:2459–2470.

Demer, D. A. 2004. An estimate of error for the CCAMLR 2000 survey estimate of krill biomass. Deep-Sea Research Part II: Topical Studies in Oceanography 51:1237–1251.

Demer, D. A., L. Berger, M. Bernasconi, E. Bethke, K. Boswell, D. Chu, R. Domokos, A. Dunford, S. Fassler, S. Gauthier, L. T. Hufnagle, J. M. Jech, N. Bouffant, A. Lebourges-Dhaussy, X. Lurton, G. J. Macaulay, Y. Perrot, T. Ryan, S. Parker-Stetter, S. Stienessen, T. Weber, and N. Williamson. 2015. Calibration of acoustic instruments.

Dormann, C. F., J. M. McPherson, M. B. Araújo, R. Bivand, J. Bolliger, G. Carl, R. G. Davies, A. Hirzel, W. Jetz, W. Daniel Kissling, I. Kühn, R. Ohlemüller, P. R. Peres-Neto, B. Reineking, B. Schröder, F. M. Schurr, and R. Wilson. 2007. Methods to account for spatial autocorrelation in the analysis of species distributional data: a review. Ecography 30:609–628.

Dulvy, N. K., S. I. Rogers, S. Jennings, V. Stelzenmüller, S. R. Dye, and H. R. Skjoldal. 2008. Climate change and deepening of the North Sea fish assemblage: a biotic indicator of warming seas. Journal of Applied Ecology 45:1029–1039.

Durham, W. M., J. O. Kessler, and R. Stocker. 2009. Disruption of vertical motility by shear triggers formation of thin phytoplankton layers. Science 323:1067–1070.

Eiane, K., and M. D. Ohman. 2004. Stage-specific mortality of *Calanus finmarchicus*, *Pseudocalanus elongatus* and *Oithona similis* on Fladen Ground, North Sea, during a spring bloom. Marine Ecology Progress Series 268:183–193.

Eigaard, O. R., M. van Deurs, J. W. Behrens, D. Bekkevold, K. Brander, M. Plambech, K. S. Plet-Hansen, and H. Mosegaard. 2014. Prey or predator—expanding the food web role of sandeel *Ammodytes marinus*. Marine Ecology Progress Series 516:267–273.

Embling, C. B., J. Illian, E. Armstrong, J. van der Kooij, J. Sharples, K. C. Camphuysen, and B. E. Scott. 2012. Investigating fine-scale spatio-temporal predator-prey patterns in dynamic marine ecosystems: A functional data analysis approach. Journal of Applied Ecology 49:481–492.

Engelhard, G. H., M. A. Peck, A. Rindorf, S. C. Smout, M. van Deurs, K. Raab, K. H. Andersen, S. Garthe, R. A. M. Lauerburg, F. Scott, T. Brunel, G. Aarts, T. van Kooten, and M. Dickey-collas. 2014. Forage fish, their fisheries, and their predators: who drives whom? ICES Journal of Marine Science 71:90–104.

Falkenhaug, T., R. Nash, K. Gundersen, S. Larsen, J. Albretsen, H. E. Heldal, and A. Hosia. 2016. North Sea Ecosystem Cruise 2015. Cruise Report. Institute of Marine Research Cruise number JH 2015204.

Fauchald, P., H. Skov, M. Skern-Mauritzen, D. Johns, and T. Tveraa. 2011. Wasp-Waist interactions in the North Sea ecosystem. PLoS ONE 6:e22729.

Fletcher, D., D. MacKenzie, and E. Villouta. 2005. Modelling skewed data with many zeros: A simple approach combining ordinary and logistic regression. Environmental and Ecological Statistics 12:45–54.

Freeman, S., S. MacKinson, and R. Flatt. 2004. Diel patterns in the habitat utilisation of sandeels revealed using integrated acoustic surveys. Journal of Experimental Marine Biology and Ecology 305:141–154.

Furness, R. W. 2002. Management implications of interactions between fisheries and sandeel-dependent seabirds and seals in the North Sea. ICES Journal of Marine Science 59:261–269.

Genin, A., J. S. Jaffe, R. Reef, C. Richter, and P. J. Franks. 2005. Swimming against the flow: A mechanism of zooplankton aggregation. Science 308:860–862.

Godø, O. R., N. O. Handegard, H. I. Browman, G. J. Macaulay, S. Kaartvedt, J. Giske, E. Ona, G. Huse, and E. Johnsen. 2014. Marine ecosystem acoustics (MEA): quantifying processes in the sea at the spatio-temporal scales on which they occur. ICES Journal of Marine Science 71:2357–2369.

Greenlaw, C. F. 1979. Acoustical estimation of zooplankton populations. Limnology and Oceanography 24:226–242.

Gregory, B., L. Christophe, and E. Martin. 2009. Rapid biogeographical plankton shifts in the North Atlantic Ocean. Global Change Biology 15:1790–1803.

Halpern, B. S., M. Frazier, J. Potapenko, K. S. Casey, K. Koenig, C. Longo, J. S. Lowndes, R. C. Rockwood, E. R. Selig, K. A. Selkoe, and S. Walbridge. 2015. Spatial and temporal changes in cumulative human impacts on the world's ocean. Nature Communications 6:1–7.

Halsband, C., and H. J. Hirche. 2001. Reproductive cycles of dominant calanoid copepods in the North Sea. Marine Ecology Progress Series 209:219–229.

Harris, V., M. Edwards, and S. C. Olhede. 2014. Multidecadal Atlantic climate variability and its impact on marine pelagic communities. Journal of Marine Systems 133:55–69.

Hjellvik, V., O. R. Godø, and D. Tjøsstheim. 2001. Modeling diurnal variation of marine populations. Biometrics 57:189–196.

Hjellvik, V., O. R. Godø, and D. Tjøstheim. 2004. Diurnal variation in acoustic densities: Why do we see less in the dark? Canadian Journal of Fisheries and Aquatic Sciences 61:2237–2254.

Hoegh-Guldberg, O., and J. F. Bruno. 2010. The impact of climate change on the world's marine ecosystems. Science 328:1523–1528.

Holmin, A. J., E. Fuglebakk, G. E. Dingsoer, A. Skaalevik, and E. Johnsen. 2019. Rstox: Running Stox functionality independently in R. https://github.com/Sea2Data/Rstox.

ICES. 2017. Report of the benchmark workshop on sandeel (WKSand 2016), 31 October−4 November 2016, Bergen. ICES CM 2016/ACOM: 33.

ICES HQ, C. 2018. Report of the Herring Assessment Working Group for the Area South of 62° N (HAWG).

Jackson, J. B. C. 2008. Ecological extinction and evolution in the brave new ocean. Proceedings of the National Academy of Sciences 105:11458–11465.

Jansen, T., and H. Gislason. 2011. Temperature affects the timing of spawning and migration of North Sea mackerel. Continental Shelf Research 31:64–72.

Jensen, H., A. Rindorf, P. J. Wright, and H. Mosegaard. 2011. Inferring the location and scale of mixing between habitat areas of lesser sandeel through information from the fishery. ICES Journal of Marine Science 68:43–51.

Johnsen, E. 2019. Råd for tobisfiskeriet i norsk sone for 2019 Tobistokt i Nordsjøen. Havforskningsinstituttet.

Johnsen, E., and O. R. Godø. 2007. Diel variations in acoustic recordings of blue whiting (*Micromesistius poutassou*). ICES Journal of Marine Science 64:1202–1209.

Johnsen, E., R. Pedersen, and E. Ona. 2009. Size-dependent frequency response of sandeel schools. ICES Journal of Marine Science 66:1100–1105.

Johnsen, E., G. Rieucau, E. Ona, and G. Skaret. 2017. Collective structures anchor massive schools of lesser sandeel to the seabed, increasing vulnerability to fishery. Marine Ecology Progress Series 573:229–236.

Jónasdóttir, S. H., and M. Koski. 2011. Biological processes in the North Sea: Comparison of *Calanus helgolandicus* and *Calanus finmarchicus* vertical distribution and production. Journal of Plankton Research 33:85–103.

Kahru, M., V. Brotas, M. Manzano-Sarabia, and B. G. Mitchell. 2011. Are phytoplankton blooms occurring earlier in the Arctic? Global Change Biology 17:1733–1739.

Kang, M., M. Furusawa, and K. Miyashita. 2002. Effective and accurate use of difference in mean volume backscattering strength to identify fish and plankton. ICES Journal of Marine Science 59:794–804.

Korneliussen, R. J., Y. Heggelund, G. J. Macaulay, D. Patel, E. Johnsen, and I. K. Eliassen. 2016. Acoustic identification of marine species using a feature library. Methods in Oceanography 17:187–205.

Korneliussen, R. J., and E. Ona. 2002. An operational system for processing and visualizing multi-frequency acoustic data. ICES Journal of Marine Science 59:293–313.

Koslow, A. J. 2009. The role of acoustics in ecosystem-based fishery management. ICES Journal of Marine Science 66:966–973.

Kubilius, R., and E. Ona. 2012. Target strength and tilt-angle distribution of the lesser sandeel (*Ammodytes marinus*). ICES Journal of Marine Science 69:1099–1107.

Lavery, A. C., P. H. Wiebe, T. K. Stanton, G. L. Lawson, M. C. Benfield, and N. Copley. 2007. Determining dominant scatterers of sound in mixed zooplankton populations. The Journal of the Acoustical Society of America 122:3304–3326.

Legendre, P. 1993. Spatial autocorrelation: trouble or new paradigm? Ecology 74:1659–1673.

Lenth, R. 2021. emmeans: Estimated marginal means, aka least-squares means. R package version 1.5.5. https://cran.r-project.org/package=emmeans.

Levine, R. M., A. De Robertis, D. Grünbaum, R. Woodgate, C. W. Mordy, F. Mueter, E. Cokelet, N. Lawrence-Slavas, and H. Tabisola. 2020. Autonomous vehicle surveys indicate that flow reversals retain juvenile fishes in a highly advective high-latitude ecosystem. Limnology and Oceanography 66:1139–1154.

Lindegren, M., M. Van Deurs, B. R. MacKenzie, L. Worsoe Clausen, A. Christensen, and A. Rindorf. 2018. Productivity and recovery of forage fish under climate change and fishing: North Sea sandeel as a case study. Fisheries Oceanography 27:212–221.

Lindegren, M., M. K. Thomas, S. H. Jónasdóttir, T. G. Nielsen, and P. Munk. 2020. Environmental niche separation promotes coexistence among ecologically similar zooplankton species—North Sea copepods as a case study. Limnology and Oceanography 65:545–556.

Mair, A. M., P. G. Fernandes, A. Lebourges-Dhaussy, and A. S. Brierley. 2005. An investigation into the zooplankton composition of a prominent 38-kHz scattering layer in the North Sea. Journal of Plankton Research 27:623–633.

Maravelias, C. D., D. G. Reid, E. J. Simmonds, and J. Haralabous. 1996. Spatial analysis and mapping of acoustic survey data in the presence of high local variability: geostatistical application to North Sea herring (*Clupea harengus*). Canadian Journal of Fisheries and Aquatic Sciences 53:1497–1505.

Mauder, M., and M. J. Zeeman. 2018. Field intercomparison of prevailing sonic anemometers. Atmospheric Measurement Techniques 11:249–263.

McManus, M. A., and C. B. Woodson. 2012. Plankton distribution and ocean dispersal. Journal of Experimental Biology 215:1008–1016.

Meinig, C., N. Lawrence-Slavas, R. Jenkins, and H. M. Tabisola. 2015. The use of Saildrones to examine spring conditions in the Bering Sea: Vehicle specification and mission performance. OCEANS 2015-MTS/IEEE Washington:IEEE.

Mordy, C. W., E. D. Cokelet, A. De Robertis, R. Jenkins, C. E. Kuhn, N. Lawrence-slavas, C. L. Berchok, J. L. Crance, J. T. Sterling, J. N. Cross, P. J. Stabeno, C. Meinig, H. M. Tabisola, W. Burgess, and I. Wangen. 2017. Advances in ecosystem research: Saildrone surveys of oceanography, fish, and marine mammals in the Bering Sea. Oceanography 30:113–115.

Perry, A. L., P. J. Low, J. R. Ellis, and J. D. Reynolds. 2005. Climate change and distribution shifts in marine fishes. Science 308:1912–1915.

Pieper, R., D. V. Holliday, and G. S. Kleppel. 1990. Quantitative zooplankton distributions from multifrequency acoustics. Journal of Plankton Research 12:433–441.

Piet, G., F. Culhane, R. Jongbloed, L. Robinson, B. Rumes, and J. Tamis. 2019. An integrated risk-based assessment of the North Sea to guide ecosystem-based management. Science of the Total Environment 654:694–704.

Pikitch, E. K., C. Santora, E. A. Babcock, A. Bakun, R. Bonfil, D. O. Conover, P. Dayton, P. Doukakis, D. Fluharty, B. Heneman, E. D. Houde, J. Link, P. A. Livingston, M. K. McAllister, J. Pope, and K. J. Sainsbury. 2004. Ecosystem-based fishery management:346–347.

Pitois, S. G., and C. J. Fox. 2006. Long-term changes in zooplankton biomass concentration and mean size over the Northwest European shelf inferred from Continuous Plankton Recorder data. ICES Journal of Marine Science 63:785–798.

Powell, J. R., and M. D. Ohman. 2015. Changes in zooplankton habitat, behavior, and acoustic scattering characteristics across glider-resolved fronts in the Southern California Current System. Progress in Oceanography 134:77–92.

Reay, P. J. 1970. Synopsis of biological data on North Atlantic sandeels of the genus Ammodytes (*A. tobianus, A. dubius, A. americanus* and *A. marinus*). Fisheries Synopsis No. 82. FAO, Rome.

Régnier, T., F. M. Gibb, and P. J. Wright. 2017. Importance of trophic mismatch in a winter-hatching species: Evidence from lesser sandeel. Marine Ecology Progress Series 567:185–197.

Shabangu, F. W., E. Ona, and D. Yemane. 2014. Measurements of acoustic attenuation at 38kHz by wind-induced air bubbles with suggested correction factors for hull-mounted transducers. Fisheries Research 151:47–56.

Simmonds, J., and D. N. MacLennan. 2008. Fisheries acoustics: theory and practice. second ed. John Wiley & Sons.

Slotte, A., K. Hansen, J. Dalen, and E. Ona. 2004. Acoustic mapping of pelagic fish distribution and abundance in relation to a seismic shooting area off the Norwegian west coast. Fisheries Research 67:143–150.

Solberg, I., T. A. Klevjer, and S. Kaartvedt. 2012. Continuous acoustic studies of overwintering sprat *sprattus sprattus* reveal flexible behavior. Marine Ecology Progress Series 464:245–256.

Stanton, T. K., P. H. Wiebe, D. Chu, M. C. Benfield, L. Scanlon, L. Martin, and R. L. Eastwood. 1994. On acoustic estimates of zooplankton biomass. ICES Journal of Marine Science 51:505–512.

Strindberg, S., and S. T. Buckland. 2004. Zigzag survey designs in line transect sampling. Journal of Agricultural, Biological, and Environmental Statistics 9:443–461.

Sundby, S., and O. Nakken. 2008. Spatial shifts in spawning habitats of Arcto-Norwegian cod related to multidecadal climate oscillations and climate change. ICES Journal of Marine Science 65:953–962.

Swart, S., J. J. Zietsman, J. C. Coetzee, D. G. Goslett, A. Hoek, D. Needham, and P. M. S.

Monteiro. 2016. Ocean robotics in support of fisheries research and management. African Journal of Marine Science 38:525–538.

Tarling, G. A., T. Jarvis, S. M. Emsley, and J. B. L. Matthews. 2002. Midnight sinking behaviour in *Calanus finmarchicus*: A response to satiation or krill predation? Marine Ecology Progress Series 240:183–194.

Thieurmel, B., and A. Elmarhraoui. 2019. Suncalc: compute sun position, sunlight phases, moon position and lunar phase. https: //CRAN.R-project.org/ package=suncalc.

Trenkel, V. M., and L. Berger. 2013. A fisheries acoustic multi-frequency indicator to inform on large scale spatial patterns of aquatic pelagic ecosystems. Ecological Indicators 30:72–79.

Trenkel, V. M., P. H. Ressler, M. Jech, M. Giannoulaki, and C. Taylor. 2011. Underwater acoustics for ecosystem-based management: state of the science and proposals for ecosystem indicators. Marine Ecology Progress Series 442:285–301.

Trevorrow, M. V. 2005. The use of moored inverted echo sounders for monitoring meso-zooplankton and fish near the ocean surface. Canadian Journal of Fisheries and Aquatic Sciences 62:1004–1018.

Urmy, S. S., J. K. Horne, and D. H. Barbee. 2012. Measuring the vertical distributional variability of pelagic fauna in Monterey Bay. ICES Journal of Marine Science 69:184–196.

Uumati, M. 2013. Acoustic investigations on bearded goby and jellyfish in the northern Benguela ecosystem (Doctoral dissertation, University of St Andrews).

van der Kooij, J., B. E. Scott, and S. Mackinson. 2008. The effects of environmental factors on daytime sandeel distribution and abundance on the Dogger Bank. Journal of Sea Research 60:201–209.

van Deurs, M., R. van Hal, M. T. Tomczak, S. H. Jónasdóttir, and P. Dolmer. 2009. Recruitment of lesser sandeel *Ammodytes marinus* in relation to density dependence and zooplankton composition. Marine Ecology Progress Series 381:249–258.

van Deurs, M., M. Koski, and A. Rindorf. 2014. Does copepod size determine food consumption of particulate feeding fish? ICES Journal ofMarine Science 71:35–43.

Verfuss, U. K., A. S. Aniceto, D. V. Harris, D. Gillespie, S. Fielding, G. Jiménez, P. Johnston, R. R. Sinclair, A. Sivertsen, S. A. Solbø, R. Storvold, M. Biuw, and R. Wyatt. 2019. A review of unmanned vehicles for the detection and monitoring of marine fauna. Marine Pollution Bulletin 140:17–29.

Visser, A. W., H. Saito, E. Saiz, and T. Kiørboe. 2001. Observations of copepod feeding and vertical distribution under natural turbulent conditions in the North Sea. Marine Biology 138:1011–1019.

Winslade, P. 1974a. Behavioural studies on the lesser sandeel *Ammodytes marinus* (Raitt) III. The effect of temperature on activity and the environmental control of the annual cycle of activity. Journal of Fish Biology 6:565–576.

Winslade, P. 1974b. Behavioural studies on the lesser sandeel *Ammodytes marinus* (Raitt) II. The effect of light intensity on activity. Journal of Fish Biology 6:577–586.

Winslade, P. 1974c. Behavioural studies on the lesser sandeel *Ammodytes marinus* (Raitt) I. The effect of food availability on activity and the role of olfaction in food detection. Journal of Fish Biology 6:565–576.

Wright, P. J., A. Christensen, T. Régnier, A. Rindorf, and M. van Deurs. 2019. Integrating the scale of population processes into fisheries management, as illustrated in the sandeel, *Ammodytes marinus*. ICES Journal of Marine Science 76:1453–1463.

Zahor, M. 2006. Acoustic identification of sandeel (*Ammodytes marinus*) using multi-

frequency methods (Doctoral dissertation, MSc thesis, Department of Biology, University of Bergen).

Zheng, M., Y. Kashimori, O. Hoshino, K. Fujita, and T. Kambara. 2005. Behavior pattern (innate action) of individuals in fish schools generating efficient collective evasion from predation. Journal of Theoretical Biology 235:153–167.

6 Appendices

6.1 Bug in LSSS version 2.9.0

A bug in LSSS version 2.9.0 was discovered during the scrutiny process of the acoustic data. Acoustic data was stored at a horizontal resolution of 0.1 nmi and a vertical resolution of 1 m in order to examine the spatial dynamics of the acoustic backscatter. The data presenting vertical distribution included small but clear cave-ins precisely every 4 m regardless of transect, depth or frequency (Figure 6.1).

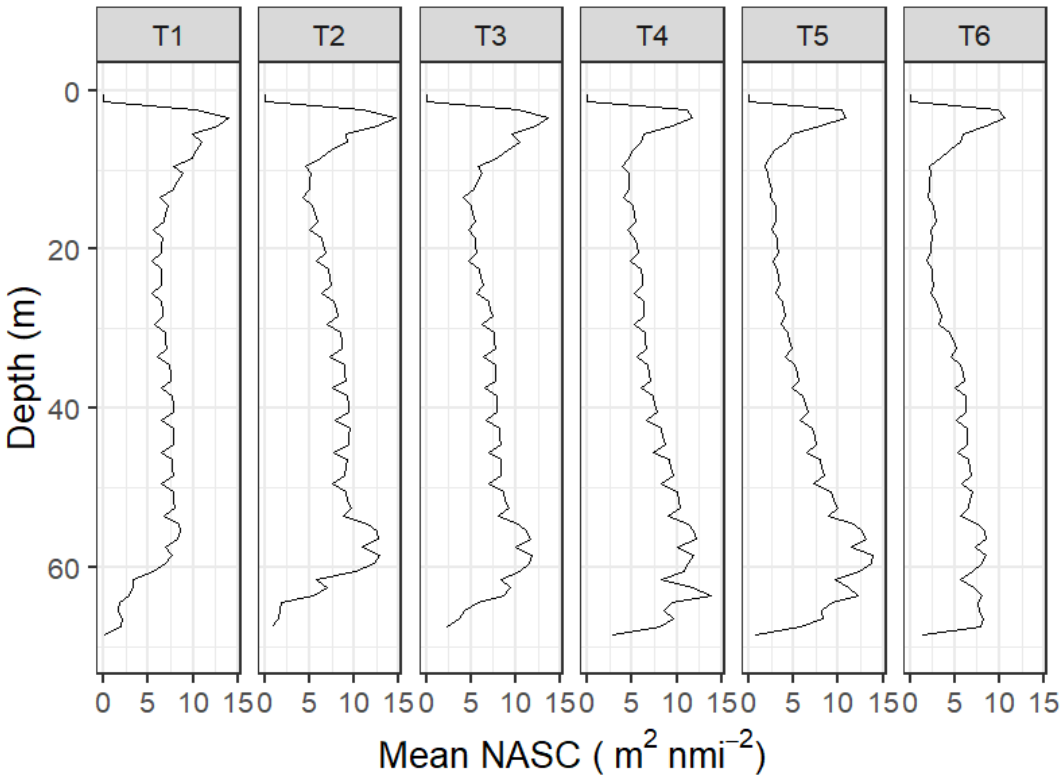

Figure 6.1. Vertical distribution of NASC at 200 kHz stored with LSSS version 2.9.0. Data from the Aberdeen-Hanstholm transect where Saildrone cruised 6 times (T1-T6) is used as an example.

Cause of the bug

This was caused by how the software integrates NASC value vertically. The raw data from echosounder fits into a pixel on a screen in the software. The pixel is the finest spatial resolution to further data manipulation and the vertical distance of a pixel is 0.17395254 m. After scrutiny,

the echogram is stored with arbitrary vertical and horizontal bins which the scrutinizer has chosen. To be stored at every 1 m in the vertical bin, 6 pixels need to be compressed into 1, which leads to 0.1734 × 6 = 1.0404 m. To counteract the excess 0.0404 m, 5 pixels are used every 4 m, which leads to 0.1734 × 5 = 0.867 m. Thus, NASC value was not computed in the same manner all the way to the bottom with the exception occurring every 4 m.

To put a theory into practice, dividing NASC value by 5 where 5 pixels were used and dividing by 6 where 6 pixels were used, the uniformized NASC value was obtained. The uniformized NASC cancelled the cave-ins every 4 m, caused by discrepancy of pixel compression, and showed smooth vertical NASC distribution (Figure 6.2).

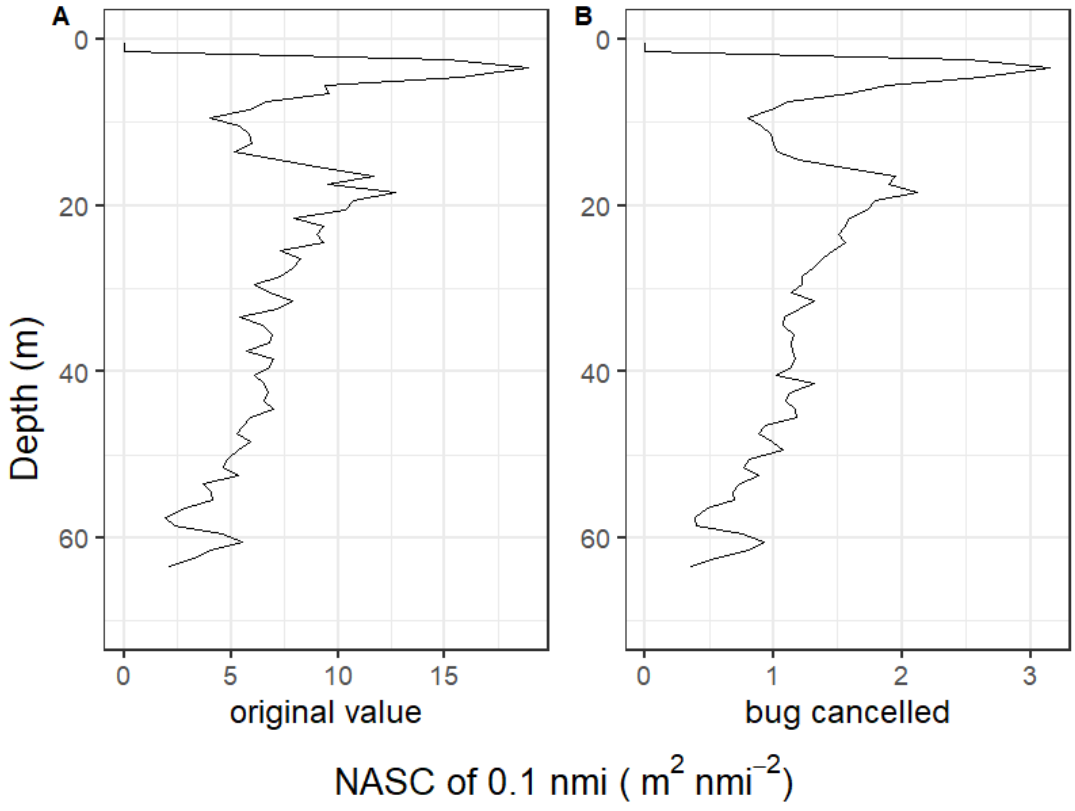

Figure 6.2. Vertical distribution of NASC at 200 kHz of 0.1 nmi (from T1 as an example) with LSSS version 2.9.0. (A) original value (B) NASC value were divided by 6 where 6 pixels were used, divided by 5 every 4 m where 5 pixels were used in order to cancel the discrepancy of pixel compression of the software.

All the data of this study was restored with the new version 2.10.0 which fixed the bug and confirmed that the 4m cave-ins had disappeared (Figure 6.3).

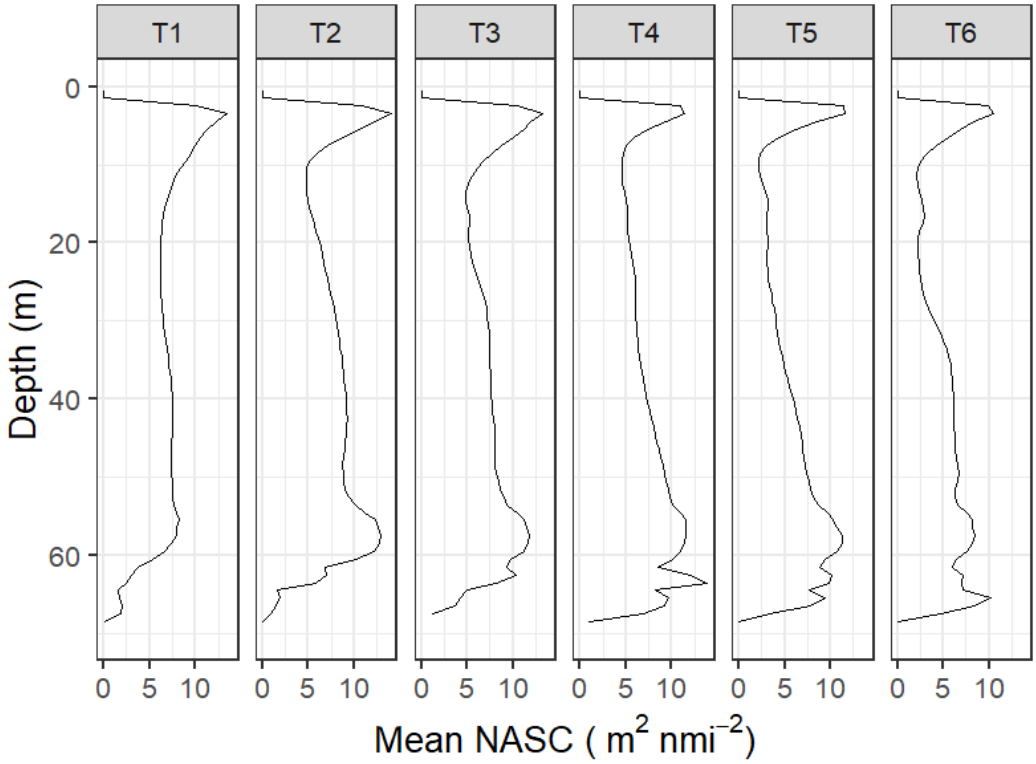

Figure 6.3. Vertical distribution of NASC at 200 kHz stored with LSSS version 2.10.0. Data from the Aberdeen-Hanstholm transect where Saildrone cruised 6 times (T1-T6) is used as an example.

Impact of the bug

The bug was detected owing to the fact that the data was stored in a finer vertical bin (1 m) in this study. The default setting of the vertical bin is 5 m in the software and many studies used the 5 m or even larger bins (Slotte et al. 2004, Johnsen and Godø 2007). The discrepancy of pixel compression ceases with larger vertical bins, making the impact of the bug insignificant. Data stored with smaller vertical bins may need to be re-examined.

6.2 Environmental factors in English Klondyke

In English Klondyke, chlorophyll and wind speed failed to collect sufficient number of samples. As a countermeasure, estimated wind speed was calculated from Saildrone cruising speed. Chlorophyll was simply removed from the analysis. Therefore, the 8 environmental factors were examined over the NASC variation at both horizontal and vertical dimensions for the non-schooling targets (Figure 6.4, Figure 6.5) in English Klondyke by means of stepwise multiple linear regression.

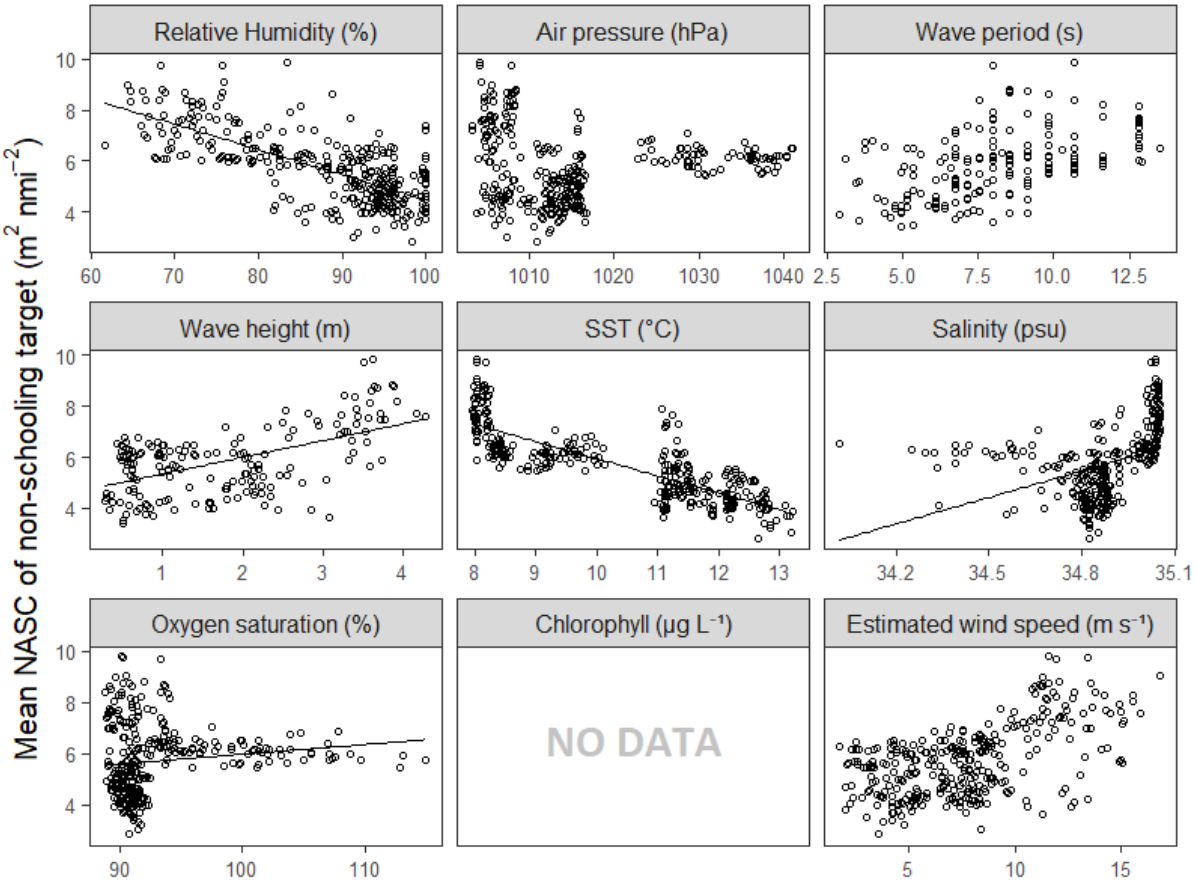

Figure 6.4. Mean NASC of the non-schooling targets at 200 kHz combining 4 coverages of English Klondyke against 8 environmental factors simultaneously recorded during the acoustic surveys. Factors which were selected via stepwise model selection contains linear regression lines. The dataset without strong backscatter in the top layer was used.

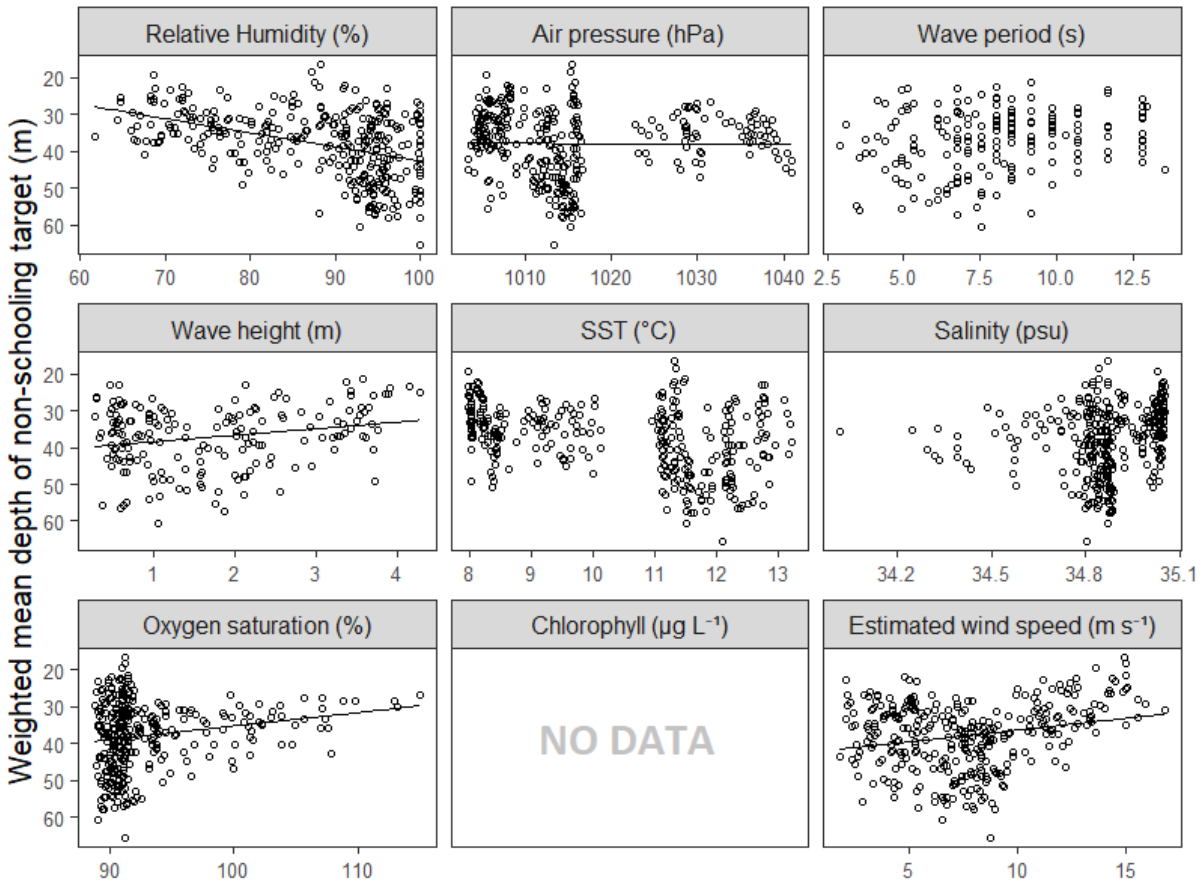

Figure 6.5. Weighted mean depth of the non-schooling targets at 200 kHz combining 4 coverages of English Klondyke against 8 environmental factors simultaneously recorded during the acoustic surveys. Factors which were selected via stepwise model selection contains linear regression lines. The dataset without strong backscatter in the top layer was used.